J. Fluid Mech. (2000), *vol.* 408, *pp.* 205–238. Printed in the United Kingdom

Using helicity to characterize homogeneous and inhomogeneous turbulent dynamics

By LEAF TURNER

Theoretical Division, Los Alamos National Laboratory, Los Alamos, NM 87545, USA

(Received 12 September 1997 and in revised form 6 December 1999)

The ability of the helicity decomposition to describe compactly the dynamics of three-dimensional incompressible fluids is invoked to obtain new descriptions of both homogeneous and inhomogeneous turbulence. We first use this decomposition to derive four coupled nonlinear equations that describe an arbitrary three-dimensional turbulence, whether anisotropic and/or non-mirror-symmetric. We then use the decomposition to treat the inhomogeneous turbulence of a channel flow bounded by two parallel free-slip boundaries with almost the ease with which the homogeneous case has heretofore received treatment. However, this ease arises from the foundation of a random-phase hypothesis, which we introduce and motivate, that supersedes the translational invariance of a turbulence that is hypothesized to be homogeneous. For the description of this channel turbulence, we find that the three-dimensional modes and the two-dimensional modes having wave vectors parallel to the boundaries each couple precisely as in a homogeneous turbulence of the corresponding dimension. The anisotropy and inhomogeneity is in large part a feature incorporated into the solenoidal basis vectors used to describe an arbitrary solenoidal free-slip flow within the channel. We invoke the random-phase hypothesis, a feature of the *dynamics*, with closures, such as Kraichnan's direct-interaction approximation and his test-field model, in addition to the one most utilized in this manuscript, the eddy-damped quasi-normal Markovian (EDQNM) closure.

1. Introduction

This is a summary of extensive work that was done several years ago (Turner 1996*a*, *b*, 1997), which is archived in the Editorial Office of this journal.

Gleaning conceptually and physically useful information concerning turbulent fluids and being able to make useful predictions about the behaviour of these fluids continue to present a couple of the finest challenges in classical physics, if not in all of physics. A mathematical model of an extremely complex nonlinear physical process is required. In this paper, we utilize a most concise notational approach, whose applicability we have extended further than previous researchers, expediting the theoretical description of (*a*) an arbitrary homogeneous incompressible turbulence – one that may be not only anisotropic but also non-mirror-symmetric – and (*b*) an incompressible turbulence in a channel flow bounded by two infinite parallel free-slip boundaries.

The mathematical foundation of our representation of the incompressible velocity field is the helical decomposition in a homogeneous geometry, which has been utilized by a legion of researchers. See, for example Herring (1974), Kraichnan (1973), Lesieur (1990*a*). Our point of embarkation is closest to that of Cambon and Waleffe. See Cambon, Teissedre & Jeandel (1985), Cambon & Jacquin (1989), Cambon, Mansour & Godeferd (1997), Waleffe (1992, 1993). The helical decomposition that, in a homogeneous geometry, is actually none other than a decomposition into right-handed (clockwise) and left-handed (counter-clockwise) polarization states of plane waves has been generalized to curvilinear geometries, such as cylindrical or spherical, by the technique of Chandrasekhar & Kendall (1957). As a result, many of the ideas and concepts here can perhaps be applied to an even greater variety of geometries than those discussed here. See, for example, Moses (1971), Montgomery, Turner & Vahala (1978), Turner & Christiansen (1981), and Turner (1983).

For fluid turbulence in a homogeneous geometry, there are only the two states associated with each wave-vector component of the solenoidal (incompressible) velocity field: a clockwise or positive-helicity state and a counter-clockwise or negative-helicity state. The reality condition on the velocity field then leads to a rank-two Hermitian matrix of the ensemble-averaged product of the quadratic moments of the velocity field at a given wave vector, $\boldsymbol{k}$. As a result, the evolution equations given by Lesieur (1990*a*) of an arbitrary homogeneous turbulence involving nine functions and nine coupled equations, in which he used the eddy-damped quasi-normal Markovian closure (EDQNM), have intrinsic linear dependences among the functions and equations that might lead to difficulties when evaluated numerically; a minimal description requires only four functions and four equations which would obviate any such difficulties.

When studying the case of fluid turbulence bounded by two infinite free-slip parallel boundaries, we found that many of the nice properties of the homogeneous basis functions would carry over to the appropriately chosen new set. The basis functions could be identified uniquely by specification of an allowed wave vector. Indeed, we found that results of the EDQNM closure look much like an amalgam of the two-dimensional isotropic homogeneous and the three-dimensional isotropic homogeneous results. The actual anisotropy and inhomogeneity is borne by the basis functions themselves through their mapping properties back into physical (coordinate) space from wave-vector space.

The loss of the theoretically restrictive, but enormously facilitating, assumption of translational invariance of the ensemble-averaged quantities is the significant problem posed by an inhomogeneous turbulence. (We shall use ‘average’ to mean ensemble-averaged.) For example, in homogeneous turbulence, the average value of the velocity covariance of an incompressible fluid is a quadratic quantity that is diagonal in the Fourier representation by virtue of the translational invariance. Were that invariance absent, any of the modes could couple to any other in a representation of the average energy. Such a situation would leave inhomogenous turbulence in an intractable state.

We are proceeding with the conventional optimism required by scientific progress. We shall assume that physical insight usefully can circumvent overwhelming and unmeasurable details through plausible approximation. We are also motivated by the knowledge that the properties of an absolute equilibrium ensemble of a truncated representation of an Euler fluid is defined by such diagonal quantities as energy for two- and three-dimensional fluids and enstrophy for a two-dimensional fluid. The cases that we shall be treating have no net kinetic helicity, which is a simplifying feature. For these flows we will posit that the large number of modes and the nonlinearity of the Navier–Stokes equation will phase-mix independent modes so that average values of quadratic quantities will be a function of only the given wave vector. We shall call this a random-phase approximation (RPA). It is an assumption about the *dynamics* of the ensemble of identical systems, not about any specific closure.

A non-zero net kinetic helicity in our representation of the fluid velocity of a channel flow would actually be non-diagonal. Thus the restriction to the case of zero kinetic helicity, though simplifying, actually may imply that our analysis has inherent limitations. Such delineation of conditions for applicability gives us optimism that our results have real significance in the applicable domain. On one hand, we are certainly not suggesting the RPA as a universal panacea for assuaging the complexities of inhomogeneous turbulence. On the other hand, our formalism has such a potential for obtaining and exploring numerical solutions to a plethora of turbulence problems, which heretofore have been unassailable, that its detailed presentation seems more worthwhile than the final equations obtained. Researchers with various interests and backgrounds can then adapt these techniques to solving their own problems.

Indeed, although most of this paper will obtain results employing the EDQNM closure, we shall conclude with pointing out that the RPA can be utilized in obtaining a variety of closures. Using the helicity decomposition and the RPA, we shall also demonstrate the direct-interaction approximation (DIA) (Kraichnan 1959) and the test-field model (TFM) (Kraichnan 1971, 1972; and Leith & Kraichnan 1972) for two- and three-dimensional turbulence as well as for the channel flow.

2. Arbitrary three-dimensional homogeneous turbulence

2.1. *The helicity decomposition of the Navier–Stokes equation*

The application of the Chandrasekhar–Kendall helicity decomposition (Chandrasekhar & Kendall 1957) to a variety of curvilinear geometries reduces to the so-called Craya representation (Craya 1958), a Fourier-based representation, for the description of incompressible velocity fields in a three-dimensional geometry. For each wave vector, $\boldsymbol{k}$, associated with the homogeneous geometry, there are two helical solenoidal states given by

$$\boldsymbol{\xi}_{\pm}(\boldsymbol{k},\boldsymbol{r}) = \hat{\boldsymbol{\chi}}_{\pm}(\boldsymbol{k})\exp(\mathrm{i}\boldsymbol{k}\cdot\boldsymbol{r}), \tag{2.1}$$

where

$$\hat{\boldsymbol{e}}^{(1)}(\boldsymbol{k}) = \frac{\hat{\boldsymbol{z}}\times\hat{\boldsymbol{k}}}{|\hat{\boldsymbol{z}}\times\hat{\boldsymbol{k}}|}, \qquad \hat{\boldsymbol{e}}^{(2)}(\boldsymbol{k}) = \hat{\boldsymbol{e}}^{(3)}(\boldsymbol{k})\times\hat{\boldsymbol{e}}^{(1)}(\boldsymbol{k}), \qquad \hat{\boldsymbol{e}}^{(3)}(\boldsymbol{k}) = \hat{\boldsymbol{k}}, \tag{2.2}$$

$$\hat{\boldsymbol{\chi}}_{\pm}(\boldsymbol{k}) = \frac{\hat{\boldsymbol{e}}^{(1)}(\boldsymbol{k})\pm\mathrm{i}\hat{\boldsymbol{e}}^{(2)}(\boldsymbol{k})}{\sqrt{2}\mathrm{i}}, \tag{2.3}$$

and where the symbol $\hat{}$ denotes a unit vector. One can verify the following properties:

$$\hat{\boldsymbol{e}}^{(1)}(-\boldsymbol{k}) = -\hat{\boldsymbol{e}}^{(1)}(\boldsymbol{k}), \qquad \hat{\boldsymbol{e}}^{(2)}(-\boldsymbol{k}) = \hat{\boldsymbol{e}}^{(2)}(\boldsymbol{k}), \qquad \hat{\boldsymbol{e}}^{(3)}(-\boldsymbol{k}) = -\hat{\boldsymbol{e}}^{(3)}(\boldsymbol{k}), \tag{2.4}$$

$$\hat{\boldsymbol{\chi}}_l^*(\boldsymbol{k}) = \hat{\boldsymbol{\chi}}_l(-\boldsymbol{k}), \qquad \hat{\boldsymbol{\chi}}_l^*(\boldsymbol{k})\cdot\hat{\boldsymbol{\chi}}_{l'}(\boldsymbol{k}) = \delta_{ll'}, \tag{2.5}$$

$$\nabla\times\boldsymbol{\xi}_l(\boldsymbol{k},\boldsymbol{r}) = s_l k\boldsymbol{\xi}_l(\boldsymbol{k},\boldsymbol{r}), \qquad \frac{1}{(2\pi)^3}\int\boldsymbol{\xi}_l^*(\boldsymbol{k}',\boldsymbol{r})\cdot\boldsymbol{\xi}_{l'}(\boldsymbol{k},\boldsymbol{r})\,\mathrm{d}^3r = \delta_{ll'}\delta^{(3)}(\boldsymbol{k}-\boldsymbol{k}'), \tag{2.6}$$

$$\boldsymbol{\xi}_l^*(\boldsymbol{k},\boldsymbol{r}) = \boldsymbol{\xi}_l(-\boldsymbol{k},\boldsymbol{r}), \tag{2.7}$$

where the subscripts l and l' take on the values $+$ or $-$, $s_{\pm} = \pm 1$, and the domain of integration is over all space. The symbol $\delta_{ll'}$ is the Kronecker delta and $\delta^{(n)}$ is the n-dimensional Dirac delta function.

We wish next to evaluate a triple-vector product, critical to the analysis of the Navier–Stokes equation in this representation; namely, the triple product $\hat{\boldsymbol{\chi}}_i(\boldsymbol{k})\cdot\hat{\boldsymbol{\chi}}_l(\boldsymbol{p})\times\hat{\boldsymbol{\chi}}_m(\boldsymbol{q})$ when $\boldsymbol{p}+\boldsymbol{q}+\boldsymbol{k} = \boldsymbol{0}$. To do so, it is useful to define the orthonormal

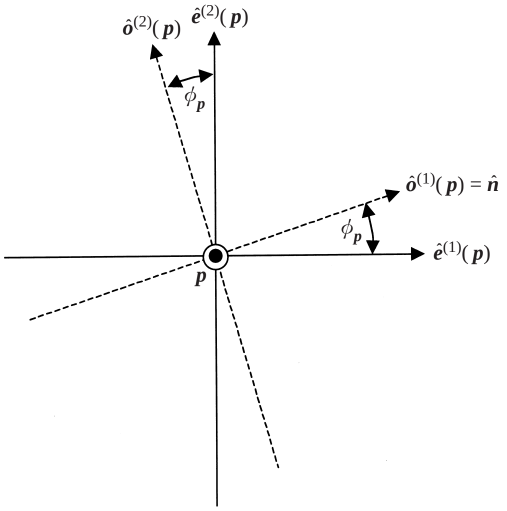

FIGURE 1. The rotation about an angle ϕ_p of the orthonormal basis vectors, $\hat{\boldsymbol{o}}^{(1)}(\boldsymbol{p})$ and $\hat{\boldsymbol{o}}^{(2)}(\boldsymbol{p})$, with respect to the orthonormal basis vectors, $\hat{\boldsymbol{e}}^{(1)}(\boldsymbol{p})$ and $\hat{\boldsymbol{e}}^{(2)}(\boldsymbol{p})$, in the plane perpendicular to $\boldsymbol{p}$. Observe that $\hat{\boldsymbol{o}}^{(1)}(\boldsymbol{p}) = \hat{\boldsymbol{n}}$.

basis vectors, $\hat{\boldsymbol{o}}^{(i)}(\boldsymbol{p})$, $i = 1, 2, 3$, by

$$\hat{\boldsymbol{o}}^{(1)}(\boldsymbol{p}) \equiv \hat{\boldsymbol{n}}, \quad \hat{\boldsymbol{o}}^{(2)}(\boldsymbol{p}) \equiv \hat{\boldsymbol{p}} \times \hat{\boldsymbol{n}}, \quad \hat{\boldsymbol{o}}^{(3)}(\boldsymbol{p}) \equiv \hat{\boldsymbol{p}}, \tag{2.8}$$

where

$$\hat{\boldsymbol{n}} \equiv \frac{\boldsymbol{k} \times \boldsymbol{p}}{|\boldsymbol{k} \times \boldsymbol{p}|} = \frac{\boldsymbol{p} \times \boldsymbol{q}}{|\boldsymbol{p} \times \boldsymbol{q}|} = \frac{\boldsymbol{q} \times \boldsymbol{k}}{|\boldsymbol{q} \times \boldsymbol{k}|}. \tag{2.9}$$

Thus the unit vector, $\hat{\boldsymbol{n}}$, is normal to the plane containing the triad of vectors, $\boldsymbol{k}, \boldsymbol{p}, \boldsymbol{q}$. In analogy to (2.3), we define

$$\hat{\boldsymbol{\Xi}}_{s_l}(\boldsymbol{k}) \equiv \frac{\hat{\boldsymbol{o}}^{(1)}(\boldsymbol{k}) + \mathrm{i}s_l\hat{\boldsymbol{o}}^{(2)}(\boldsymbol{k})}{\sqrt{2}\mathrm{i}}. \tag{2.10}$$

Figure 1 shows that

$$\hat{\boldsymbol{\chi}}_l(\boldsymbol{k}) = \exp(\mathrm{i}s_l\phi_k)\hat{\boldsymbol{\Xi}}_l(\boldsymbol{k}), \tag{2.11}$$

where

$$\cos(\phi_k) \equiv \hat{\boldsymbol{o}}^{(1)}(\boldsymbol{k}) \cdot \hat{\boldsymbol{e}}^{(1)}(\boldsymbol{k}) = \hat{\boldsymbol{n}} \cdot \hat{\boldsymbol{e}}^{(1)}(\boldsymbol{k}), \tag{2.12}$$

$$\sin(\phi_k) \equiv \hat{\boldsymbol{o}}^{(1)}(\boldsymbol{k}) \cdot \hat{\boldsymbol{e}}^{(2)}(\boldsymbol{k}) = \hat{\boldsymbol{n}} \cdot \hat{\boldsymbol{e}}^{(2)}(\boldsymbol{k}). \tag{2.13}$$

One then can verify that

$$\hat{\boldsymbol{\chi}}_i(\boldsymbol{k}) \cdot \hat{\boldsymbol{\chi}}_l(\boldsymbol{p}) \times \hat{\boldsymbol{\chi}}_m(\boldsymbol{q}) = -\frac{\mathrm{i}s_is_ls_m \exp[\mathrm{i}(s_i\phi_k + s_l\phi_p + s_m\phi_q)_{\hat{\boldsymbol{n}}(\boldsymbol{k},\boldsymbol{p},\boldsymbol{q})}]}{(2)^{3/2}} \times (s_i \sin\alpha_k + s_l \sin\alpha_p + s_m \sin\alpha_q). \tag{2.14}$$

The labelled arguments of the sin's are the angles of the kpq-triangle where the subscript on a given α is the label of the side opposite that angle. See figure 2. These angles result from the relation $\hat{\boldsymbol{n}} \cdot \hat{\boldsymbol{p}} \times \hat{\boldsymbol{q}} = \sin\alpha_k$, as well as those obtained from cyclic permution of the vectors: $\boldsymbol{k} \rightarrow \boldsymbol{p} \rightarrow \boldsymbol{q} \rightarrow \boldsymbol{k}$. If now we utilize both this helicity

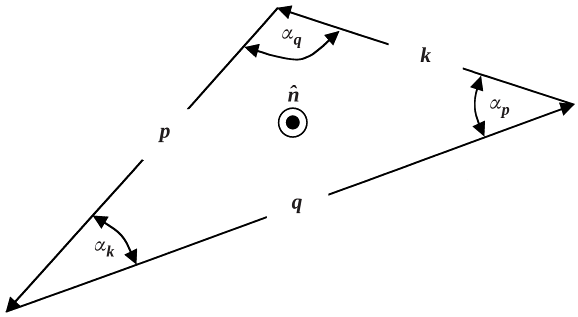

FIGURE 2. The relative orientation of the triad of wave vectors, $\boldsymbol{k}$, $\boldsymbol{p}$, and $\boldsymbol{q}$. The angles are labelled with subscripts specifying the opposite sides. Note also that $\hat{\boldsymbol{n}}$ is perpendicular to the plane of the triad and has the orientation shown.

decomposition to represent the velocity field,

$$\boldsymbol{u}(\boldsymbol{r},t)=\sum_{i=\pm}\int \mathrm{d}^3k\, c_i(\boldsymbol{k},t)\boldsymbol{\xi}_i(\boldsymbol{k},\boldsymbol{r}), \tag{2.15}$$

and the Navier–Stokes equation,

$$\frac{\partial \boldsymbol{u}(\boldsymbol{r},t)}{\partial t}+\boldsymbol{u}(\boldsymbol{r},t)\cdot\nabla\boldsymbol{u}(\boldsymbol{r},t)=-\nabla p(\boldsymbol{r},t)+\nu\nabla^2\boldsymbol{u}(\boldsymbol{r},t), \tag{2.16}$$

we can insert this representation of the velocity and of the concomitant vorticity (the curl of the velocity field) into the curl of the Navier–Stokes equation in which the pressure field no longer appears. Utilizing the orthonormality of the basis functions, we obtain the equation determining the time evolution of the spectral coefficients:

$$\begin{aligned}\left(\frac{\partial}{\partial t}+\nu k^2\right)c_i(\boldsymbol{k},t)=\frac{1}{2}\int \mathrm{d}^3q\,\mathrm{d}^3p\,\delta^{(3)}(\boldsymbol{k}-\boldsymbol{p}-\boldsymbol{q})\\ \times\sum_{l,m=\pm}(s_mq-s_lp)c_l(\boldsymbol{p},t)c_m(\boldsymbol{q},t)M_{ilm}(-\boldsymbol{k},\boldsymbol{p},\boldsymbol{q}),\end{aligned} \tag{2.17}$$

where $M_{ilm}(\boldsymbol{k},\boldsymbol{p},\boldsymbol{q})\equiv\hat{\boldsymbol{\chi}}_i(\boldsymbol{k})\cdot\hat{\boldsymbol{\chi}}_l(\boldsymbol{p})\times\hat{\boldsymbol{\chi}}_m(\boldsymbol{q})$, which is displayed in (2.14). Using the law of sines for triangles and Heron's formula for the area of the triangle, $A(k,p,q)$, we equally well can represent M as

$$M_{ilm}(\boldsymbol{k},\boldsymbol{p},\boldsymbol{q})=-\mathrm{i}\frac{A(k,p,q)s_is_ls_m\exp\left[\mathrm{i}(s_i\phi_{\boldsymbol{k}}+s_l\phi_{\boldsymbol{p}}+s_m\phi_{\boldsymbol{q}})_{\hat{\boldsymbol{n}}(\boldsymbol{k},\boldsymbol{p},\boldsymbol{q})}\right]}{\sqrt{2}kpq}(s_ik+s_lp+s_mq), \tag{2.18}$$

in which $A(k,p,q)=[h(h-k)(h-p)(h-q)]^{1/2}$ where h is half the perimeter of the kpq-triangle, i.e. $h=(k+p+q)/2$.

Using (2.17) and (2.18), we also can write the evolution equation of the spectral coefficients using the *structure function*, g_{ilm}, as

$$\left(\frac{\partial}{\partial t}+\nu k^2\right)c_i(\boldsymbol{k},t)=\int \mathrm{d}^3q\,\mathrm{d}^3p\sum_{l,m=\pm}c_l(\boldsymbol{p},t)c_m(\boldsymbol{q},t)g_{ilm}(-\boldsymbol{k},\boldsymbol{p},\boldsymbol{q}), \tag{2.19}$$

where

$$g_{ilm}(\boldsymbol{k},\boldsymbol{p},\boldsymbol{q})=(s_mq-s_lp)\frac{M_{ilm}(\boldsymbol{k},\boldsymbol{p},\boldsymbol{q})}{2}\delta^{(3)}(\boldsymbol{k}+\boldsymbol{p}+\boldsymbol{q}). \tag{2.20}$$

2.2. *Evolution of the turbulent spectrum for homogeneous turbulence*

We are now poised to develop the EDQNM equation for the evolution of this homogeneous turbulence.

We shall refer to the second-rank tensor quantity, $\boldsymbol{U}(\boldsymbol{k},t)$, as the turbulent spectrum. It is defined by

$$\langle c_j(\boldsymbol{k},t)c_i(\boldsymbol{k}',t)\rangle \equiv \delta^{(3)}(\boldsymbol{k}+\boldsymbol{k}')U_{ji}(\boldsymbol{k},t), \tag{2.21}$$

where the notation, $\langle\ \rangle$, denotes an ensemble-averaged quantity. Using the reality condition, which assures the real nature of the physical fluid velocity,

$$c_i(\boldsymbol{k},t) = c_i^*(-\boldsymbol{k},t), \tag{2.22}$$

one can verify that

$$\boldsymbol{U}(\boldsymbol{k},t) = \boldsymbol{U}^\dagger(\boldsymbol{k},t) = \boldsymbol{U}^T(-\boldsymbol{k},t), \tag{2.23}$$

where the † and the T superscripts denote the Hermitian conjugate and the transpose operations, respectively, on the matrix $\boldsymbol{U}$. One can think of the elements of $\boldsymbol{U}$ as being given by

$$U_{ji}(\boldsymbol{k},t) = \hat{\boldsymbol{\chi}}_j^*(\boldsymbol{k})\cdot\boldsymbol{U}(\boldsymbol{k},t)\cdot\hat{\boldsymbol{\chi}}_i(\boldsymbol{k}). \tag{2.24}$$

Perhaps the efficiency of notation of the helicity decomposition is most readily displayed in the derivation of the equations that describe the statistical evolution of any arbitrary homogeneous turbulence of a constant-density fluid. Instead of our having to keep track of the nine matrix elements of the usual Fourier transform of the velocity–velocity correlation, we need to keep track of only four elements. The constraint of solenoidality, which is ordinarily maintained through the byzantine use of transverse projection operators, is automatically guaranteed by the helicity decomposition at the outset without further ado.

The four elements have been extensively utilized by Cambon and his co-workers (Cambon & Jacquin 1989; Cambon *et al.* 1997) to study rotating turbulence, for which this helical-mode decomposition is well-adapted. In their notation, the matrix $\boldsymbol{U}(\boldsymbol{k},t)$ can be written as:

$$\boldsymbol{U}(\boldsymbol{k},t) = \left\{\begin{array}{cc} e(\boldsymbol{k},t) + \dfrac{h(\boldsymbol{k},t)}{k} & -Z^*(\boldsymbol{k},t) \\ -Z(\boldsymbol{k},t) & e(\boldsymbol{k},t) - \dfrac{h(\boldsymbol{k},t)}{k} \end{array}\right\}, \tag{2.25}$$

in which they call $Z(\boldsymbol{k},t)$ the polarization anisotropy. The functions, $e(\boldsymbol{k},t)$ and $h(\boldsymbol{k},t)$, are the energy and kinetic helicity.

Obtaining the equation for the time-evolution of an arbitrary anisotropic homogeneous turbulence – even in the presence of mirror asymmetry – in an incompressible one-component fluid using the eddy-damped quasi-normal Markovian (EDQNM) closure entails a great deal of algebra. Along the way, one introduces the eddy-damped closure that expresses the third-order moment of the spectral coefficients, $T_{ilm}(\boldsymbol{k},\boldsymbol{p},\boldsymbol{q},t)$, (defined as $\langle c_i(\boldsymbol{k},t)c_l(\boldsymbol{p},t)c_m(\boldsymbol{q},t)\rangle$) in terms of matrix elements of the $\boldsymbol{U}$ in the following manner:

$$\begin{aligned} T_{ilm}(\boldsymbol{k},\boldsymbol{p},\boldsymbol{q},t) = \theta(k,p,q;t) \sum_{i',l',m'=\pm} & M^*_{i'l'm'}(\boldsymbol{k},\boldsymbol{p},\boldsymbol{q})\{(s_{i'}k - s_{m'}q) \\ & \times U_{mm'}(\boldsymbol{q},t)[U_{ii'}(\boldsymbol{k},t)\delta_{ll'} - U_{ll'}(\boldsymbol{p},t)\delta_{ii'}] \\ & + (s_{l'}p - s_{i'}k)U_{ll'}(\boldsymbol{p},t)[U_{ii'}(\boldsymbol{k},t)\delta_{mm'} - U_{mm'}(\boldsymbol{q},t)\delta_{ii'}]\}, \end{aligned} \tag{2.26}$$

in which $\theta(k,p,q;t)$ is the heuristically motivated eddy-damping function. The final equation for the evolution of the spectrum then follows:

$$\begin{aligned}\frac{\partial U_{ij}(\boldsymbol{k},t)}{\partial t}+2\nu k^2U_{ij}(\boldsymbol{k},t)=\frac{1}{2}\int\frac{\mathrm{d}^3p\mathrm{d}^3q}{k^2p^2q^2}\delta^{(3)}(\boldsymbol{k}+\boldsymbol{p}+\boldsymbol{q})\theta(k,p,q;t)A^2(k,p,q)\\ \times\Big(\Big\{\{[2(k^2-q^2)(q^2-p^2)\Lambda_4^{\hat{\boldsymbol{n}}}(\boldsymbol{q},t)s_i+2kq(k^2-q^2)\Lambda_1^{\hat{\boldsymbol{n}}}(\boldsymbol{q},t)\\ +2kqp^2\Lambda_2^{\hat{\boldsymbol{n}}}(\boldsymbol{q},t)]\sum_{j'=\pm}s_{j'}\tilde{U}^{\hat{\boldsymbol{n}}}_{j'j}(\boldsymbol{k},t)-2k^2p^2\Lambda_4^{\hat{\boldsymbol{n}}}(\boldsymbol{q},t)\\ \times\sum_{j'=\pm}\tilde{U}^{\hat{\boldsymbol{n}}}_{j'j}(\boldsymbol{k},t)+\tfrac{1}{2}(q^2-p^2)^2\Lambda_4^{\hat{\boldsymbol{n}}}(\boldsymbol{p},t)\Lambda_4^{\hat{\boldsymbol{n}}}(\boldsymbol{q},t)s_is_j\\ +kq(q^2-p^2)\Lambda_4^{\hat{\boldsymbol{n}}}(\boldsymbol{p},t)[\Lambda_2^{\hat{\boldsymbol{n}}}(\boldsymbol{q},t)s_i+\Lambda_1^{\hat{\boldsymbol{n}}}(\boldsymbol{q},t)s_j]\\ +k^2q^2\Lambda_4^{\hat{\boldsymbol{n}}}(\boldsymbol{p},t)\Lambda_0^{\hat{\boldsymbol{n}}}(\boldsymbol{q},t)-k^2pq\Lambda_2^{\hat{\boldsymbol{n}}}(\boldsymbol{p},t)\Lambda_1^{\hat{\boldsymbol{n}}}(\boldsymbol{q},t)\}\\ \times\exp\,[i(s_j-s_i)\phi_{\boldsymbol{k}}]_{\hat{\boldsymbol{n}}(\boldsymbol{k},\boldsymbol{p},\boldsymbol{q})}\Big\}+\{i\leftrightarrow j\}^*\Big).\end{aligned}\tag{2.27}$$

The final bracket implies that one is to add a term obtained from the first bracket by interchanging i and j and taking the complex conjugate. The turbulence is defined here by means of $\boldsymbol{U}(\boldsymbol{k},t)$, a two-dimensional Hermitian matrix (see (2.21, 2.23)) to which the functions, $\Lambda_0^{\hat{\boldsymbol{n}}},\Lambda_1^{\hat{\boldsymbol{n}}},\Lambda_2^{\hat{\boldsymbol{n}}},\Lambda_4^{\hat{\boldsymbol{n}}}$, and the two-dimensional Hermitian matrix, $\tilde{\boldsymbol{U}}^{\hat{\boldsymbol{n}}}$, are related as follows:

$$\tilde{U}^{\hat{\boldsymbol{n}}}_{lm}(\boldsymbol{p},t)\equiv\exp\,(is_l\phi_{\boldsymbol{p}})_{\hat{\boldsymbol{n}}(\boldsymbol{k},\boldsymbol{p},\boldsymbol{q})}U_{lm}(\boldsymbol{p},t)\exp\,(-\mathrm{i}s_m\phi_{\boldsymbol{p}})_{\hat{\boldsymbol{n}}(\boldsymbol{k},\boldsymbol{p},\boldsymbol{q})},\tag{2.28}$$

$$\Lambda_0^{\hat{\boldsymbol{n}}}(\boldsymbol{p},t)\equiv\sum_{l,m}\tilde{U}^{\hat{\boldsymbol{n}}}_{lm}(\boldsymbol{p},t),\qquad \Lambda_1^{\hat{\boldsymbol{n}}}(\boldsymbol{p},t)\equiv\sum_{l,m}s_l\tilde{U}^{\hat{\boldsymbol{n}}}_{lm}(\boldsymbol{p},t),\tag{2.29}$$

$$\Lambda_2^{\hat{\boldsymbol{n}}}(\boldsymbol{p},t)\equiv\sum_{l,m}s_m\tilde{U}^{\hat{\boldsymbol{n}}}_{lm}(\boldsymbol{p},t),\qquad \Lambda_4^{\hat{\boldsymbol{n}}}(\boldsymbol{p},t)\equiv\sum_{l,m}s_ls_m\tilde{U}^{\hat{\boldsymbol{n}}}_{lm}(\boldsymbol{p},t).\tag{2.30}$$

Equation (2.27) is the EDQNM equation that specifies the evolution of an arbitrary anisotropic homogeneous turbulence. Thus four equations involving only four real scalar functions specify the dynamics of an arbitrary anisotropic homogeneous turbulence that need not even be mirror-symmetric. Calculation with these four equations would be more efficient than with those nine equations of Lesieur (1990*a*) involving nine scalar functions that possess latent, but intrinsic, linear dependences. To glean additional understanding of the four elements of $\boldsymbol{U}(\boldsymbol{k},t)$, see Cambon & Jacquin (1989).

2.3. *Isotropic homogeneous Navier–Stokes turbulence: A test-case for EDQNM*

For the case of isotropic homogeneous turbulence, the tensor $\boldsymbol{U}$ must be a function of only the magnitude of the wave vector and take the form

$$U_{ij}(\boldsymbol{k},t)=\delta_{ij}U_i(k,t)=\frac{\delta_{ij}}{4\pi k^2}[E(k,t)+s_ik^{-1}H(k,t)].\tag{2.31}$$

The evolution equations for the energy and helicity spectra that we obtain (Turner 1996*a*) from (2.27) for this case of isotropic turbulence are precisely those obtained by André & Lesieur (1977).

Orszag (1977) has demonstrated quite simply that in the absence of any viscosity and when the kinetic helicity spectrum vanishes, the only equilibrium solution of the

EDQNM evolution equation for the energy spectrum is an equipartition spectrum. Kraichnan (1973) has specified the spectrum of an absolute equilibrium ensemble for the truncated inviscid Navier–Stokes equation (i.e. the Euler equation) with non-zero kinetic helicity. Since the EDQNM evolution equation is only an approximation of reality that continues to be utilized, it is encumbent on us to validate its predictions as much as possible. In particular, we shall now verify that the unique equilibrium (steady-state) solution to the truncated, inviscid form of (2.27) is Kraichnan's absolute equilibrium ensemble.

To do so, we first observe that the right-hand side of (2.26) has the factor, $F(k,p,q)$, where

$$F(k,p,q) = (s_i k - s_m q)U_m(q)U_i(k) + (s_l p - s_i k)U_i(k)U_l(p) + (s_m q - s_l p)U_l(p)U_m(q). \tag{2.32}$$

Then, dividing by the product of the three spectral components on the right-hand side, we readily observe

$$\frac{F(k,p,q)}{U_i(k)U_l(p)U_m(q)} = \frac{s_i k - s_m q}{U_l(p)} + \frac{s_l p - s_i k}{U_m(q)} + \frac{s_m q - s_l p}{U_i(k)}. \tag{2.33}$$

We can represent each denominator on the right-hand side of this equation using

$$U_l^{-1}(p) = g_1(p) + s_l g_2(p), \tag{2.34}$$

where

$$g_1(p) = \frac{1}{2}\sum_{l=\pm} U_l^{-1}(p), \qquad g_2(p) = \frac{1}{2}\sum_{l=\pm} s_l U_l^{-1}(p). \tag{2.35}$$

Then,

$$\begin{aligned}\frac{F(k,p,q)}{U_i(k)U_l(p)U_m(q)} &= s_i k[g_1(p) - g_1(q)] + s_l p[g_1(q) - g_1(k)] \\ &+ s_m q[g_1(k) - g_1(p)] + s_i s_l[k g_2(p) - p g_2(k)] \\ &+ s_l s_m[p g_2(q) - q g_2(p)] + s_m s_i[q g_2(k) - k g_2(q)]. \end{aligned} \tag{2.36}$$

We next can assure the vanishing of $T_{ilm}(\boldsymbol{k},\boldsymbol{p},\boldsymbol{q},t)$ by imposing the condition that $F(k,p,q)$ vanish. Thus an equilibrium solution is obtained by setting

$$g_1(k) = g_1(p) = g_1(q) = \alpha, \qquad \frac{g_2(k)}{k} = \frac{g_2(p)}{p} = \frac{g_2(q)}{q} = -\beta, \tag{2.37}$$

where α and β are constants. Therefore,

$$U_i(k) = \frac{1}{\alpha - s_i \beta k}. \tag{2.38}$$

Using (2.31), we find that

$$E(k) = \frac{4\pi k^2 \alpha}{\alpha^2 - \beta^2 k^2}, \qquad H(k) = \frac{4\pi k^3 \beta}{\alpha^2 - \beta^2 k^2}, \tag{2.39}$$

which is precisely the absolute equilibrium ensemble spectrum in the presence of kinetic helicity obtained by Kraichnan (1973).

Since the equations of the EDQNM constitute a statistical closure, they necessarily entail a loss of detail. Nevertheless, it is to the credit of the EDQNM approximation that the only equilibrium solution of the truncated representation of the Euler equation in the presence of both isotropy and *kinetic helicity* is the absolute equilibrium ensemble of Kraichnan, despite the intricate dynamics engendered by the presence of the kinetic helicity!

3. Bounded three-dimensional turbulence: the free-slip channel

3.1. *Introduction*

The hallmark of all practical fluid turbulence problems, from the streamlining of transportation vehicles, combustion in automotive engines, and flow through turbines, to meteorological and astrophysical phenomena, and even to eruptions of volcanoes and forest fires, is their inhomogeneous nature. Because gradients of such fundamental quantities as the mean pressure, mean velocity, pressure–velocity, and triple-velocity correlations are necessarily absent in homogeneous models but universally present in these physically realistic situations, any attempt at fathoming such neglected aspects of inhomogeneous turbulence ought to be a high-priority subject for research – one that should stimulate great curiosity and excitement. Although for reasons of mathematical simplicity we shall focus on the case of free-slip boundary conditions to demonstrate the effectiveness of our approach, there should be no fundamental obstacle intrinsic to this approach that would prevent its application to other boundary conditions, such as no-slip, or to other bounded geometries, such as cylindrical or spherical. For example, see Chandrasekhar & Kendall (1957), Moses (1971), Montgomery *et al.* (1978), Turner & Christiansen (1981), Turner (1983), Chandrasekhar & Reid (1957), Li, Montgomery & Jones (1996, 1997).

Therefore, the case of free-slip parallel boundaries confining a Navier–Stokes turbulence is of interest for three reasons: first, because its methodology is a prototype for the more complicated cases just enumerated; second, because this methodology uses tools whose teeth have already been well-honed on the case of homogeneous turbulence; and third, because we have a consistent tool with which to answer inhomogeneous turbulence questions. The random-phase approximation that we employ has recently been well-verified by means of comparison with direct numerical simulations of Navier–Stokes turbulence in the absence of mean flows (Ulitsky, Clark & Turner 1999; Turner & Turner 2000). Probably the weakest aspect of our calculation when compared with the analogous calculations of homogeneous turbulence is the choice of our eddy-damping function, $\theta(k, p, q; t)$, as will be discussed in § 3.5. Nevertheless, our procedure has not been prejudiced by use of any preconceptions of desired phenomenology. The pressure field is non-locally determined through Poisson's equation being implicitly satisfied. Thus we are calculating physical quantities involving dynamics significantly complicated by the bounded geometry, but without any necessity for simplifying assumptions of restrictive symmetries such as homogeneity and isotropy.

Previous researchers of inhomogeneous turbulence often made the assumption that the spatial inhomogeneity was weak. See Bertoglio & Jeandel (1987), Schiestel (1987), Besnard *et al.* (1996). For example, suppose one were examining a two-point correlation, say $c(\boldsymbol{r}_1, \boldsymbol{r}_2)$. One can think of the correlation as a function of the variables $\boldsymbol{r}_+ = (\boldsymbol{r}_1 + \boldsymbol{r}_2)/2$ and $\boldsymbol{r}_- = (\boldsymbol{r}_1 - \boldsymbol{r}_2)/2$. The assumption of weak inhomogeneity that is used is that the dependence of c on $\boldsymbol{r}_+$ is gentle, i.e. one needs to consider only very few terms in a Taylor series expansion of c in $\boldsymbol{r}_+$ about some value of the $\boldsymbol{r}_+$-variable. We make no assumption of weak inhomogeneity.

3.2. *The helicity decomposition for the channel flow*

The boundary conditions on fluid velocity and vorticity appropriate to a free-slip boundary are

$$\boldsymbol{v}\cdot\hat{\boldsymbol{n}} = \boldsymbol{0}, \qquad \boldsymbol{\omega}\times\hat{\boldsymbol{n}} = \boldsymbol{0}, \tag{3.1}$$

where these equations are evaluated at the boundary and where the unit vector $\hat{\boldsymbol{n}}$ is normal to the boundary. Because of the required vanishing of the normal component of the velocity, the second constraint is equivalent to the requirement that there be no stress imposed on the fluid at the boundary.

We shall assume that the boundaries are located at $y = 0$ and at $y = L_y$. We shall also assume periodic boundary conditions along the $\hat{\boldsymbol{x}}$- and $\hat{\boldsymbol{z}}$-directions parallel to the boundary with periodicity lengths L_x and L_z, respectively. We define the wave vectors, $\boldsymbol{k}_\pm$ by

$$\boldsymbol{k}_\pm \equiv \left(\frac{2\pi l}{L_x}, \pm\frac{\pi m}{L_y}, \frac{2\pi n}{L_z}\right), \tag{3.2}$$

where we shall use the notation that $\boldsymbol{k} = \boldsymbol{k}_+$.

We then represent the fluid velocity, $\boldsymbol{u}(\boldsymbol{r}, t)$, as a sum over the following set of solenoidal basis vectors:

$$\boldsymbol{u}(\boldsymbol{r}, t) = V_0\hat{\boldsymbol{z}} + \sum_{\boldsymbol{k}} c_{\boldsymbol{k}}(t)\boldsymbol{\varDelta}(\boldsymbol{k}, \boldsymbol{r}). \tag{3.3}$$

These vectors are defined by

$$\boldsymbol{\varDelta}(\boldsymbol{k}, \boldsymbol{r}) \equiv \frac{[\boldsymbol{\xi}_+(\boldsymbol{k}_+, \boldsymbol{r}) - \boldsymbol{\xi}_-(\boldsymbol{k}_-, \boldsymbol{r})]}{2}, \tag{3.4}$$

and satisfy

$$\nabla\times\boldsymbol{\varDelta}(\boldsymbol{k}, \boldsymbol{r}) = k\boldsymbol{\sigma}(\boldsymbol{k}, \boldsymbol{r}), \tag{3.5}$$

where

$$\boldsymbol{\sigma}(\boldsymbol{k}, \boldsymbol{r}) \equiv \frac{[\boldsymbol{\xi}_+(\boldsymbol{k}_+, \boldsymbol{r}) + \boldsymbol{\xi}_-(\boldsymbol{k}_-, \boldsymbol{r})]}{2}. \tag{3.6}$$

As in § 2.1, when $\boldsymbol{k} \nparallel \hat{\boldsymbol{z}}$, we define

$$\hat{\boldsymbol{e}}^{(1)}(\boldsymbol{k}) \equiv \frac{\hat{\boldsymbol{z}}\times\hat{\boldsymbol{k}}}{|\hat{\boldsymbol{z}}\times\hat{\boldsymbol{k}}|}. \tag{3.7}$$

When $\boldsymbol{k} \parallel \hat{\boldsymbol{z}}$, we set

$$\hat{\boldsymbol{e}}^{(1)}(\boldsymbol{k}) \equiv \operatorname{sgn}(k_z)\hat{\boldsymbol{y}}. \tag{3.8}$$

In either case, we maintain the definition

$$\hat{\boldsymbol{e}}^{(2)}(\boldsymbol{k}) \equiv \hat{\boldsymbol{k}}\times\hat{\boldsymbol{e}}^{(1)}(\boldsymbol{k}). \tag{3.9}$$

One sees that the vorticity is simply

$$\boldsymbol{\omega}(\boldsymbol{r}, t) = \sum_{\boldsymbol{k}} kc_{\boldsymbol{k}}(t)\boldsymbol{\sigma}(\boldsymbol{k}, \boldsymbol{r}). \tag{3.10}$$

The $\boldsymbol{\sigma}$s satisfy

$$\nabla\times\boldsymbol{\sigma}(\boldsymbol{k}, \boldsymbol{r}) = k\boldsymbol{\varDelta}(\boldsymbol{k}, \boldsymbol{r}). \tag{3.11}$$

The basis vectors satisfy the appropriate free-slip condition on the boundaries at $y = 0$ and at $y = L_y$,

$$\boldsymbol{\varDelta}(\boldsymbol{k}, \boldsymbol{r})\cdot\hat{\boldsymbol{y}} = 0, \qquad \boldsymbol{\sigma}(\boldsymbol{k}, \boldsymbol{r})\times\hat{\boldsymbol{y}} = \boldsymbol{0}, \tag{3.12}$$

as well as the reality condition,

$$\boldsymbol{\Delta}^*(\boldsymbol{k},\boldsymbol{r}) = \boldsymbol{\Delta}(-\boldsymbol{k},\boldsymbol{r}), \qquad \boldsymbol{\sigma}^*(\boldsymbol{k},\boldsymbol{r}) = \boldsymbol{\sigma}(-\boldsymbol{k},\boldsymbol{r}). \tag{3.13}$$

They are orthonormal within each set:

$$\frac{2}{L_x L_y L_z}\int \mathrm{d}^3r\boldsymbol{\Delta}^*(\boldsymbol{k},\boldsymbol{r})\cdot\boldsymbol{\Delta}(\boldsymbol{k}',\boldsymbol{r}) = \frac{2}{L_x L_y L_z}\int \mathrm{d}^3r\boldsymbol{\sigma}^*(\boldsymbol{k},\boldsymbol{r})\cdot\boldsymbol{\sigma}(\boldsymbol{k}',\boldsymbol{r}) = \delta_{\boldsymbol{k},\boldsymbol{k}'}. \tag{3.14}$$

A consequence of the reality of the fluid velocity and the condition (3.13) is

$$c^*(\boldsymbol{k},t) = c(-\boldsymbol{k},t). \tag{3.15}$$

3.3. *The energy spectrum and two-point velocity autocorrelation*

We are now set to obtain the evolution equation for the turbulence of our bounded channel flow. Without loss of generality because of Galilean invariance, we shall always be assuming that $V_0 = 0$ in (3.3). As in the homogeneous case above, we commence by taking the curl of the Navier–Stokes equation. We then can use the properties of our representation summarized in the previous section to obtain an equation for the time evolution of the spectral coefficients. The only tricky part is the evaluation of the integral over the triple vector product of the basis functions. This is most readily accomplished by expanding the solenoidal basis vectors out in terms of their $\boldsymbol{\xi}$-components, as given in (3.4) and (3.6), and then utilizing the results of §2.1 for the triple product of the $\boldsymbol{\xi}$ vectors. We thereby obtain a nonlinear equation for the evolution of the coefficients, again of the form

$$\left(\frac{\partial}{\partial t} + \nu k^2\right) c(\boldsymbol{k},t) = \sum_{\boldsymbol{k}_1,\boldsymbol{k}_2} c(\boldsymbol{k}_1,t)c(\boldsymbol{k}_2,t)g(\boldsymbol{k}_1,\boldsymbol{k}_2,-\boldsymbol{k}), \tag{3.16}$$

in which

$$g(\boldsymbol{k}_1,\boldsymbol{k}_2,-\boldsymbol{k}) \equiv \frac{2}{L_x L_y L_z}\int \mathrm{d}^3r\boldsymbol{\Delta}(-\boldsymbol{k},\boldsymbol{r})\cdot\left[\frac{\boldsymbol{\Delta}(\boldsymbol{k}_1,\boldsymbol{r})\times\boldsymbol{\sigma}(\boldsymbol{k}_2,\boldsymbol{r})k_2 + \boldsymbol{\Delta}(\boldsymbol{k}_2,\boldsymbol{r})\times\boldsymbol{\sigma}(\boldsymbol{k}_1,\boldsymbol{r})k_1}{2}\right]. \tag{3.17}$$

The structure function, $g(\boldsymbol{k},\boldsymbol{p},\boldsymbol{q})$, implicitly contains all of the dynamical and geometric information involved in the bounded flow. It satisfies the following symmetry properties:

$$g(\boldsymbol{k},\boldsymbol{p},\boldsymbol{q}) = g(\boldsymbol{p},\boldsymbol{k},\boldsymbol{q}), \tag{3.18}$$

$$g(\boldsymbol{k},\boldsymbol{p},\boldsymbol{q}) + g(\boldsymbol{p},\boldsymbol{q},\boldsymbol{k}) + g(\boldsymbol{q},\boldsymbol{k},\boldsymbol{p}) = 0, \tag{3.19}$$

$$g^*(\boldsymbol{k},\boldsymbol{p},\boldsymbol{q}) = g(-\boldsymbol{k},-\boldsymbol{p},-\boldsymbol{q}). \tag{3.20}$$

The final expression for the structure function is

$$\begin{aligned} g(\boldsymbol{k},\boldsymbol{p},\boldsymbol{q}) = {} & \frac{\delta_{k_x+p_x+q_x,0}\delta_{k_z+p_z+q_z,0}}{4}\left[\frac{-\mathrm{i}A(k,p,q)}{\sqrt{2}kpq}\right] \\ & \times\{\delta_{p_y+k_y+q_y,0}\exp[\mathrm{i}(\phi_{\boldsymbol{k}_+}+\phi_{\boldsymbol{p}_+}+\phi_{\boldsymbol{q}_+})_{\hat{\boldsymbol{n}}(\boldsymbol{k}_+,\boldsymbol{p}_+,\boldsymbol{q}_+)}](p+k+q)(p-k) \\ & +\delta_{p_y+k_y-q_y,0}\exp[\mathrm{i}(\phi_{\boldsymbol{k}_+}+\phi_{\boldsymbol{p}_+}-\phi_{\boldsymbol{q}_-})_{\hat{\boldsymbol{n}}(\boldsymbol{k}_+,\boldsymbol{p}_+,\boldsymbol{q}_-)}](p+k-q)(p-k) \\ & +\delta_{p_y-k_y-q_y,0}\exp[\mathrm{i}(\phi_{\boldsymbol{k}_+}-\phi_{\boldsymbol{p}_-}+\phi_{\boldsymbol{q}_+})_{\hat{\boldsymbol{n}}(\boldsymbol{k}_+,\boldsymbol{p}_-,\boldsymbol{q}_+)}](p-k-q)(p+k) \\ & +\delta_{p_y-k_y+q_y,0}\exp[\mathrm{i}(-\phi_{\boldsymbol{k}_-}+\phi_{\boldsymbol{p}_+}+\phi_{\boldsymbol{q}_+})_{\hat{\boldsymbol{n}}(\boldsymbol{k}_-,\boldsymbol{p}_+,\boldsymbol{q}_+)}](p-k+q)(p+k)\}. \end{aligned} \tag{3.21}$$

In the development of the EDQNM closure for the Navier–Stokes turbulence arising from (3.16), we shall encounter ensemble averages of the quadratic product of spectral coefficients; namely $\langle c(\boldsymbol{k},t)c(\boldsymbol{k}',t)\rangle$. When $\boldsymbol{k}' = -\boldsymbol{k}$, we define the scalar function of $\boldsymbol{k}$

$$U(\boldsymbol{k},t) \equiv \langle c(\boldsymbol{k},t)c(-\boldsymbol{k},t)\rangle. \tag{3.22}$$

In the absence of any specific constraints on the ensemble and by virtue of both the nonlinear character of the Navier–Stokes equation as well as the large number of modes and the apparently random (or chaotic) nature of physical turbulence, we suggest that the spectral coefficients in (3.16) may be assumed to have phases that are uncorrelated with each other in the restricted sense that

$$\langle c(\boldsymbol{k},t)c(\boldsymbol{k}',t)\rangle = U(\boldsymbol{k},t)\delta_{\boldsymbol{k},-\boldsymbol{k}'}. \tag{3.23}$$

This assumption is also consistent with what would be expected for the quadratic correlations of an absolute equilibrium ensemble that has no mean kinetic helicity.

We shall refer to (3.23) as the restricted *random phase approximation* (RPA). Its validity, which is independent of any statistical closure, may be checked by direct numerical simulations (Ulitsky *et al.* 1999; Turner & Turner 2000). Note that unlike the assumption of spatial homogeneity, our assumption of restricted random phase does not imply the vanishing of $\langle c(\boldsymbol{k}_1,t)c(\boldsymbol{k}_2,t)\cdots c(\boldsymbol{k}_n,t)\rangle$ when $\boldsymbol{k}_1+\boldsymbol{k}_2+\cdots+\boldsymbol{k}_n \neq 0$ except when $n = 2$. Indeed the RPA has nothing whatever to do with spatial homogeneity. Its meaning in physical space is inherent in the expansion basis associated with the specific boundary conditions and geometry under consideration. Furthermore, there should be no reason why one cannot apply the RPA to boundary conditions other than free-slip. For example, one might conceive of an orthogonal set of solenoidal basis vectors appropriate for describing no-slip boundary conditions, some two- or three-dimensional generalization, say, of the Chandrasekhar–Reid functions (Chandrasekhar & Reid 1957). See also Li *et al.* (1996, 1997).

Random phase approximations have been successfully employed in other areas of physics. See, for example, Bohm & Pines (1951). (Despite the plausibility of this assumption, *caveat emptor!* For example, one should not use this assumption when additional constraints on the ensemble exist, such as the presence of a non-zero ensemble-averaged kinetic helicity in the fluctuations, because a direct consequence of the RPA in the slab geometry is the absence of any ensemble-averaged kinetic helicity in the fluctuations!) Of course, when the turbulence is approximated as homogeneous, the associated translational invariance implies the validity of the RPA.

Observe that (3.15) and (3.22) imply that

$$U(\boldsymbol{k},t) = U(-\boldsymbol{k},t) = U^*(\boldsymbol{k},t). \tag{3.24}$$

Thus $U(\boldsymbol{k},t)$ must be a real, non-negative scalar function of the vector $\boldsymbol{k}$. Using the orthonormality of the $\boldsymbol{\Delta}(\boldsymbol{k},\boldsymbol{r})$, (3.14), yields

$$\frac{2}{L_xL_yL_z}\int \mathrm{d}^3r\, u^2(\boldsymbol{r},t) = \sum_{\boldsymbol{k}} U(\boldsymbol{k},t). \tag{3.25}$$

We see then that $U(\boldsymbol{k},t)$ is the energy spectrum defined by our solenoidal basis. We shall be assuming that

$$U(\boldsymbol{k}_+,t) = U(\boldsymbol{k}_-,t). \tag{3.26}$$

This condition can be shown to maintain the vanishing of the ensemble-averaged values of the fluctuations, i.e. $\langle c(\boldsymbol{k},t)\rangle = 0$. See Turner (1996*b*).

A consequence of the symmetry properties of the energy spectrum, (3.24), and the RPA is that we can immediately obtain the two-point velocity correlation tensor for our spectral components:

$$\begin{aligned}\langle \boldsymbol{u}(\boldsymbol{R}+\tfrac{1}{2}\boldsymbol{r},t)\boldsymbol{u}(\boldsymbol{R}-\tfrac{1}{2}\boldsymbol{r},t)\rangle &= \frac{1}{4}\sum_{\boldsymbol{k}} U(\boldsymbol{k},t)\\ &\quad\times[\boldsymbol{\Delta}^*(\boldsymbol{k},\boldsymbol{R}+\tfrac{1}{2}\boldsymbol{r})\boldsymbol{\Delta}(\boldsymbol{k},\boldsymbol{R}-\tfrac{1}{2}\boldsymbol{r})+\boldsymbol{\Delta}^*(-\boldsymbol{k},\boldsymbol{R}+\tfrac{1}{2}\boldsymbol{r})\boldsymbol{\Delta}(-\boldsymbol{k},\boldsymbol{R}-\tfrac{1}{2}\boldsymbol{r})\\ &\quad+\boldsymbol{\Delta}^*(\boldsymbol{k}_-,\boldsymbol{R}+\tfrac{1}{2}\boldsymbol{r})\boldsymbol{\Delta}(\boldsymbol{k}_-,\boldsymbol{R}-\tfrac{1}{2}\boldsymbol{r})+\boldsymbol{\Delta}^*(-\boldsymbol{k}_-,\boldsymbol{R}+\tfrac{1}{2}\boldsymbol{r})\boldsymbol{\Delta}(-\boldsymbol{k}_-,\boldsymbol{R}-\tfrac{1}{2}\boldsymbol{r})]\\ &= \sum_{\boldsymbol{k}} U(\boldsymbol{k},t)\boldsymbol{S}(\boldsymbol{R}+\tfrac{1}{2}\boldsymbol{r},\boldsymbol{R}-\tfrac{1}{2}\boldsymbol{r};\boldsymbol{k}). \end{aligned}\tag{3.27}$$

Performing the evaluations, we find the following results for the matrix elements:

$$\left.\begin{aligned}
S_{11}(\boldsymbol{R}+\tfrac{1}{2}\boldsymbol{r},\boldsymbol{R}-\tfrac{1}{2}\boldsymbol{r};\boldsymbol{k}) &= \tfrac{1}{2}(1-k_x^2/k^2)\cos(k_y y_\Delta)\cos(k_y y_\sigma)\cos(\boldsymbol{k}_\parallel\cdot\boldsymbol{r}_\parallel),\\
S_{21}(\boldsymbol{R}+\tfrac{1}{2}\boldsymbol{r},\boldsymbol{R}-\tfrac{1}{2}\boldsymbol{r};\boldsymbol{k}) &= \frac{k_xk_y}{2k^2}\cos(k_y y_\Delta)\sin(k_y y_\sigma)\sin(\boldsymbol{k}_\parallel\cdot\boldsymbol{r}_\parallel),\\
S_{31}(\boldsymbol{R}+\tfrac{1}{2}\boldsymbol{r},\boldsymbol{R}-\tfrac{1}{2}\boldsymbol{r};\boldsymbol{k}) &= -\frac{k_xk_z}{2k^2}\cos(k_y y_\Delta)\cos(k_y y_\sigma)\cos(\boldsymbol{k}_\parallel\cdot\boldsymbol{r}_\parallel),\\
S_{12}(\boldsymbol{R}+\tfrac{1}{2}\boldsymbol{r},\boldsymbol{R}-\tfrac{1}{2}\boldsymbol{r};\boldsymbol{k}) &= -\frac{k_xk_y}{2k^2}\sin(k_y y_\Delta)\cos(k_y y_\sigma)\sin(\boldsymbol{k}_\parallel\cdot\boldsymbol{r}_\parallel),\\
S_{22}(\boldsymbol{R}+\tfrac{1}{2}\boldsymbol{r},\boldsymbol{R}-\tfrac{1}{2}\boldsymbol{r};\boldsymbol{k}) &= \frac{1}{2}\left(1-\frac{k_y^2}{k^2}\right)\sin(k_y y_\Delta)\sin(k_y y_\sigma)\cos(\boldsymbol{k}_\parallel\cdot\boldsymbol{r}_\parallel),\\
S_{32}(\boldsymbol{R}+\tfrac{1}{2}\boldsymbol{r},\boldsymbol{R}-\tfrac{1}{2}\boldsymbol{r};\boldsymbol{k}) &= -\frac{k_yk_z}{2k^2}\sin(k_y y_\Delta)\cos(k_y y_\sigma)\sin(\boldsymbol{k}_\parallel\cdot\boldsymbol{r}_\parallel),\\
S_{13}(\boldsymbol{R}+\tfrac{1}{2}\boldsymbol{r},\boldsymbol{R}-\tfrac{1}{2}\boldsymbol{r};\boldsymbol{k}) &= -\frac{k_xk_z}{2k^2}\cos(k_y y_\Delta)\cos(k_y y_\sigma)\cos(\boldsymbol{k}_\parallel\cdot\boldsymbol{r}_\parallel),\\
S_{23}(\boldsymbol{R}+\tfrac{1}{2}\boldsymbol{r},\boldsymbol{R}-\tfrac{1}{2}\boldsymbol{r};\boldsymbol{k}) &= \frac{k_yk_z}{2k^2}\cos(k_y y_\Delta)\sin(k_y y_\sigma)\sin(\boldsymbol{k}_\parallel\cdot\boldsymbol{r}_\parallel),\\
S_{33}(\boldsymbol{R}+\tfrac{1}{2}\boldsymbol{r},\boldsymbol{R}-\tfrac{1}{2}\boldsymbol{r};\boldsymbol{k}) &= \frac{1}{2}\left(1-\frac{k_z^2}{k^2}\right)\cos(k_y y_\Delta)\cos(k_y y_\sigma)\cos(\boldsymbol{k}_\parallel\cdot\boldsymbol{r}_\parallel);
\end{aligned}\right\}\tag{3.28}$$

where

$$y_\Delta \equiv Y-\frac{y}{2},\quad y_\sigma\equiv Y+\frac{y}{2},\quad \boldsymbol{k}_\parallel\cdot\boldsymbol{r}_\parallel = k_xx+k_zz,\tag{3.29}$$

and where

$$\left.\begin{aligned}&\boldsymbol{R}\equiv(X,Y,Z),\quad \boldsymbol{r}=(x,y,z),\\ &k_x\equiv\frac{2\pi l}{L_x},\quad k_y\equiv\frac{\pi m}{L_y},\quad k_z\equiv\frac{2\pi n}{L_z}.\end{aligned}\right\}\tag{3.30}$$

We are using the subscripts, 1, 2, and 3 to refer to the ordinary Cartesian components in the x-, y-, and z-directions, respectively.

One should note that the structure of this matrix exhibits vestiges of the structure of the two-point velocity autocorrelation matrix for homogeneous isotropic turbulence, which has its diagonal ii-elements proportional to $(1 - k_i^2/k^2)$. In § 3.4, we shall see further vestiges of the homogeneous isotropic turbulent dynamics.

One should note also that

$$\langle u^2(\boldsymbol{R},t)\rangle = \sum_{\boldsymbol{k}} U(\boldsymbol{k},t) \sum_{i=1}^{3} S_{ii}(\boldsymbol{R},\boldsymbol{R};\boldsymbol{k}) = \sum_{\boldsymbol{k}} \frac{U(\boldsymbol{k},t)}{2}\left[1 + \frac{k_y^2}{k^2}\cos(2k_y Y)\right]. \quad (3.31)$$

Therefore, a surprising consequence of the RPA in the presence of free-slip boundary conditions is that the value of the turbulent kinetic energy of the fluid at the planar boundaries equals or exceeds its value at any point within those boundaries.

Before ending discussion of this tensor, one should observe that owing to the symmetry of slab turbulence, the mean pressure has a gradient oriented in the y-direction. Using the Navier–Stokes equation and the incompressibility of the flow, one observes that the 22-element is the source of the gradient because

$$\frac{\partial\langle p(\boldsymbol{r},t)\rangle}{\partial y} = -\langle \boldsymbol{u}(\boldsymbol{r},t)\cdot\nabla u_y(\boldsymbol{r},t)\rangle = -\nabla\cdot\langle \boldsymbol{u}(\boldsymbol{r},t)u_y(\boldsymbol{r},t)\rangle = -\frac{\partial\langle u_y^2(\boldsymbol{r},t)\rangle}{\partial y}.$$

Thus,

$$\frac{\partial\langle p(\boldsymbol{r},t) + u_y^2(\boldsymbol{r},t)\rangle}{\partial y} = 0. \quad (3.32)$$

Since u_y must vanish at the boundaries, we see that in the immediate neighbourhood of the boundaries the mean pressure must not decrease as the point of interest moves toward the boundaries.

3.4. *Evolution of the turbulent spectrum for channel flow*

Proceeding to derive the evolution equation for the turbulent spectrum for the channel flow using the RPA and the EDQNM closure, we obtain

$$\left[\frac{\partial}{\partial t} + 2\nu k^2\right] U(\boldsymbol{k},t) = \left\{4\sum_{\boldsymbol{k}_1,\boldsymbol{k}_2} g(\boldsymbol{k}_1,\boldsymbol{k}_2,\boldsymbol{k})(g(-\boldsymbol{k},-\boldsymbol{k}_1,-\boldsymbol{k}_2)U(\boldsymbol{k}_1,t) \times[U(\boldsymbol{k},t) - U(\boldsymbol{k}_2,t)]\theta(\boldsymbol{k},\boldsymbol{k}_1,\boldsymbol{k}_2;t)\right\} + \{\boldsymbol{k} \Leftrightarrow -\boldsymbol{k}\}, \quad (3.33)$$

in which the phenomenological eddy-damping function is assumed to be a totally symmetric function of its wave-vector arguments and to satisfy

$$\theta(\boldsymbol{k},\boldsymbol{k}',\boldsymbol{k}'';t) = \theta(-\boldsymbol{k},-\boldsymbol{k}',-\boldsymbol{k}'';t) = \theta(\boldsymbol{k}_-,\boldsymbol{k}'_-,\boldsymbol{k}''_-;t). \quad (3.34)$$

We shall be saying more about our choice for this function in § 3.5.

One can prove that this evolution equation has the following properties:

(*a*) if the initial energy spectrum satisfies the symmetry, $U(\boldsymbol{k},0) = U(\boldsymbol{k}_-,0)$, then it retains this symmetry as it evolves, namely for all time $U(\boldsymbol{k},t) = U(\boldsymbol{k}_-,t)$;

(*b*) it produces a realizable energy spectrum, namely if, as is required by definition, for all $\boldsymbol{k}$, $U(\boldsymbol{k},0) \geqslant 0$, then it retains the property $U(\boldsymbol{k},t) \geqslant 0$ for arbitrary $\boldsymbol{k}$ and all time; and

(*c*) an equipartition energy spectrum, i.e. a $\boldsymbol{k}$-independent $U(\boldsymbol{k},t)$, is an equilibrium spectrum in the inviscid limit. This trivially obtainable result is not surprising for an ensemble having no net kinetic helicity.

We shall massage (3.33) into a form that manifests well-known aspects of both two- and three-dimensional homogeneous turbulence, *although the turbulence under consideration is inhomogeneous.*

The three-dimensional aspect can be extracted from the coupling between three modes whose wave vectors, $\boldsymbol{k}, \boldsymbol{p}$, and $\boldsymbol{q}$, all have non-vanishing y-components, i.e. $k_y p_y q_y \neq 0$. First, observe that the product of the two structure functions in (3.33) (after replacing the dummy variables $\boldsymbol{k}_1$ and $\boldsymbol{k}_2$ by $\boldsymbol{p}$ and $\boldsymbol{q}$, respectively) has only four surviving terms, namely

$$\begin{aligned} g^*(\boldsymbol{k},\boldsymbol{p},\boldsymbol{q})g(\boldsymbol{p},\boldsymbol{q},\boldsymbol{k}) &= \delta_{k_x+p_x+q_x,0}\delta_{k_z+p_z+q_z,0}\frac{A^2(k,p,q)}{32k^2p^2q^2} \\ &\quad\times \sum_{s_p,s_q=\pm} \delta_{k_y+s_pp_y+s_qq_y,0}(k+s_pp+s_qq)^2(k-s_pp)(s_pp-s_qq). \end{aligned} \tag{3.35}$$

Because the energy spectra which multiply this term in the EDQNM evolution equation are insensitive to the signs of the y-components of the wave vectors, we can replace this result by the ansatz

$$\begin{aligned} g^*(\boldsymbol{k},\boldsymbol{p},\boldsymbol{q})g(\boldsymbol{p},\boldsymbol{q},\boldsymbol{k}) &\to \delta_{k_x+p_x+q_x,0}\delta_{k_y+p_y+q_y,0}\delta_{k_z+p_z+q_z,0}\frac{A^2(k,p,q)}{32k^2p^2q^2} \\ &\quad\times \sum_{s_p,s_q=\pm} [(p^2-q^2)+k(s_pp-s_qq)][(k^2-p^2)+s_qq(k-s_pp)] \\ &= \delta_{\boldsymbol{k}+\boldsymbol{p}+\boldsymbol{q},\boldsymbol{0}}\frac{A^2(k,p,q)}{8}[(p^2-q^2)(k^2-p^2)-k^2q^2] \end{aligned} \tag{3.36}$$

prior to insertion into the right-hand side of the evolution equation. The expression $\delta_{\boldsymbol{k}+\boldsymbol{p}+\boldsymbol{q},\boldsymbol{0}}$ is used to represent the product $\delta_{k_x+p_x+q_x,0}\ \delta_{k_y+p_y+q_y,0}\ \delta_{k_z+p_z+q_z,0}$.

The two-dimensional aspect can be extracted from the coupling between three modes whose wave vectors, $\boldsymbol{k}, \boldsymbol{p}$, and $\boldsymbol{q}$, all have vanishing y-components; that is, $k_y = p_y = q_y = 0$. First, observe that this is a degenerate case in which all four terms contributing to each of the two structure functions in (3.33) (after replacing the dummy variables, $\boldsymbol{k}_1$ and $\boldsymbol{k}_2$ by $\boldsymbol{p}$ and $\boldsymbol{q}$, respectively) survive. To evaluate the exponential factors, notice that the normal vector, $\hat{\boldsymbol{n}}(\boldsymbol{k},\boldsymbol{p},\boldsymbol{q}) = s_c\hat{\boldsymbol{y}}$, where s_c takes on the value $+1$ or -1, depending on the orientation of the kpq-triad of vectors in the (x,z)-plane (counterclockwise or clockwise, respectively, when looking in the $-\boldsymbol{y}$-direction toward the triad). Using (2.12) and (2.13), one may verify that $\exp(\mathrm{i}\phi_{\boldsymbol{k}}) = s_c\,\mathrm{sgn}\,(k_x)$, with precisely analogous expressions for $\exp(\mathrm{i}\phi_{\boldsymbol{p}})$ and $\exp(\mathrm{i}\phi_{\boldsymbol{q}})$. Thus when $k_y = p_y = q_y = 0$, we may use (3.21) to obtain

$$g(\boldsymbol{k},\boldsymbol{p},\boldsymbol{q}) = \delta_{k_x+p_x+q_x,0}\delta_{k_z+p_z+q_z,0}\left[\frac{-\mathrm{i}A(k,p,q)}{\sqrt{2}kpq}\right](p^2-k^2)\,\mathrm{sgn}\,(s_ck_xp_xq_x). \tag{3.37}$$

Hence we obtain the following result for the product of the two structure functions when the y-components of all three wave vectors vanish:

$$g^*(\boldsymbol{k},\boldsymbol{p},\boldsymbol{q})g(\boldsymbol{p},\boldsymbol{q},\boldsymbol{k}) = \delta_{k_x+p_x+q_x,0}\delta_{k_z+p_z+q_z,0}\left[\frac{A(k,p,q)^2}{2k^2p^2q^2}\right](k^2-p^2)(p^2-q^2). \tag{3.38}$$

We thereby arrive at the following final EDQNM-RPA evolution equation for inhomogeneous turbulence of our free-slip bounded fluid:

$$\left[\frac{\partial}{\partial t}+2\nu k^2\right]U(\boldsymbol{k},t)=\sum_{\boldsymbol{p},\boldsymbol{q}\ni p_y q_y\neq 0}\delta_{\boldsymbol{k},\boldsymbol{p}+\boldsymbol{q}}\frac{A^2(k,p,q)}{k^2p^2q^2}[(k^2-p^2)(q^2-p^2)+k^2q^2]$$
$$\times\theta(\boldsymbol{k},\boldsymbol{p},\boldsymbol{q};t)U(\boldsymbol{p},t)[U(\boldsymbol{q},t)-U(\boldsymbol{k},t)]$$
$$+\delta_{k_y,0}\sum_{\boldsymbol{p},\boldsymbol{q}\ni p_y=q_y=0}\delta_{k_x,p_x+q_x}\delta_{k_z,p_z+q_z}\frac{4A^2(k,p,q)}{k^2p^2q^2}(k^2-p^2)(q^2-p^2)$$
$$\times\theta(\boldsymbol{k},\boldsymbol{p},\boldsymbol{q};t)U(\boldsymbol{p},t)[U(\boldsymbol{q},t)-U(\boldsymbol{k},t)]$$
$$+\text{hybrid contributions.} \tag{3.39}$$

The third term on the right-hand side of (3.39), denoted *hybrid contributions*, refers to those combinations of terms in which one of the y-components of the three wave vectors, $\boldsymbol{k},\boldsymbol{p}$, or $\boldsymbol{q}$, is zero, each of the other two y-components being non-zero. What is amazing is that the wave-vector space coupling of the first term on the right-hand side of this equation for the evolution of slab turbulence is precisely that expected for the evolution of isotropic, mirror-symmetric, homogeneous three-dimensional turbulence, while at the same time the coupling of the second term on the right-hand side is precisely that expected for the evolution of isotropic, mirror-symmetric, homogeneous two-dimensional turbulence (Leith & Kraichnan 1972)! Yet observe that even if our spectrum, $U(\boldsymbol{k},t)$, is isotropic in wave-vector space (i.e. depends only on the magnitude of the wave vector $\boldsymbol{k}$), the mapping from wave-vector space back to physical space will be neither homogeneous nor isotropic!

3.5. *Numerical results for channel flow*

We wish to display and discuss some results that we have numerically obtained using (3.39). We used as our initial ($t=0$) spectral distribution

$$U(\boldsymbol{k},0)=k^2\exp\left(-\frac{k^2}{2}\right). \tag{3.40}$$

We used the following length scales: $L_x=L_z=50, L_y=25$ in order that when $l=m=n$, $k_x=k_y=k_z$. We used a kinematic viscosity, $\nu=0.5$. The integer values of l,m, and n specifying the modes ranged from -20 to 20. We chose the following phenomenological form for the eddy-damping function, $\theta(\boldsymbol{k},\boldsymbol{p},\boldsymbol{q};t)$:

$$\theta(\boldsymbol{k},\boldsymbol{p},\boldsymbol{q};t)=[\nu(k^2+p^2+q^2)+\tilde{\mu}(k,t)+\tilde{\mu}(p,t)+\tilde{\mu}(q,t)]^{-1}, \tag{3.41}$$

where

$$\tilde{\mu}(k,t)=\left[\sum_{\boldsymbol{k}'\ni k'\leqslant k}k'^2U(\boldsymbol{k}',t)\right]^{1/2}. \tag{3.42}$$

The arguments normally used to motivate this choice of θ for spatially homogeneous turbulence clearly no longer apply. Nevertheless, we maintain this form of θ for several reasons: first, simplicity – at present we have no reason, say, from direct numerical simulations, to motivate a more complicated choice such as a non-unity constant preceding the square bracket on the right-hand side of the expression defining $\tilde{\mu}(k,t)$; second, we wish to keep our analysis as close as possible to the analysis employed in earlier studies in order to be able to make useful comparisons; third, we are making a choice that reduces to a term proportional to the conventional EDQNM for two-

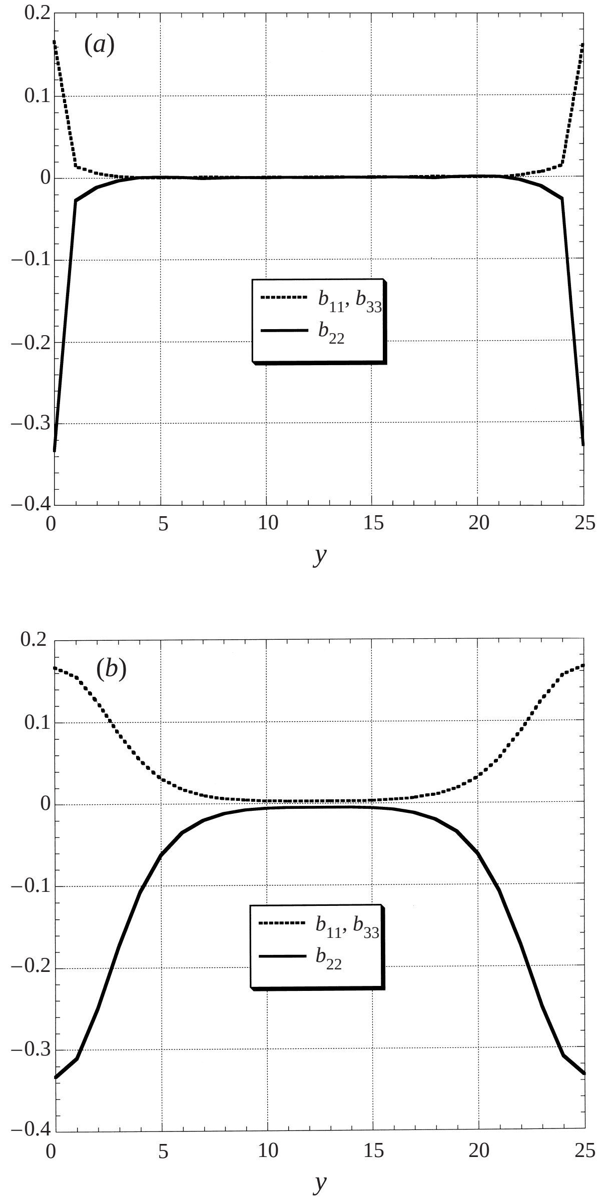

FIGURE 3. Non-vanishing elements of the normalized anisotropy tensor, b_{ij}, as a function of y. The free-slip boundaries are located at $y = 0$ and at $y = 25$: (a) $t = 0.92$, (b) $t = 12.0$.

dimensional fluid turbulence (Leith & Kraichnan 1972). The only way it would be possible to make a more informed choice regarding the structure of θ would be to have information gleaned from direct numerical simulations or from a more detailed turbulence theory. The simplest such theory would be the test-field model. See §4.3. There we would have approximately $(2N)^9$ differential equations (perhaps divided by 4^3 to account for the symmetries of the spectrum, $U(\boldsymbol{k}, t) = U(-\boldsymbol{k}, t) = U(\boldsymbol{k}_-, t)$), describing the evolution of θ as a function of the three components of its three wave-vector arguments, in which $N = 20$ for the current calculation. Thus use of the test-field model directly would be computationally prohibitive.

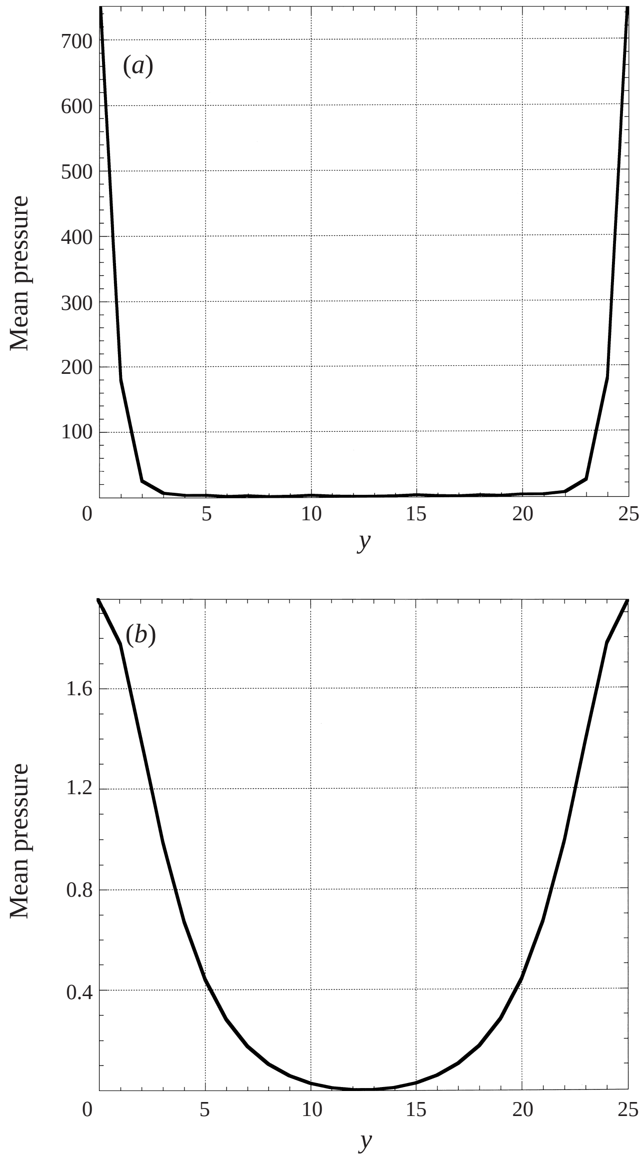

FIGURE 4. The associated mean pressure profiles where we have represented the pressures using the gauge in which the mean pressure at the midpoint, $y = 12.5$, is zero: (a) $t = 0.92$, (b) $t = 12.0$.

In figure 3, we display the normalized anisotropic velocity autocorrelation tensor, b_{ij}, where $b_{ij}(y) \equiv r_{ij}(y) - \delta_{ij}/3$. The normalized velocity autocorrelation is defined by $r_{ij}(y) \equiv \langle \boldsymbol{u}(\boldsymbol{r})\boldsymbol{u}(\boldsymbol{r})\rangle_{ij}/\mathrm{Tr}\langle \boldsymbol{u}(\boldsymbol{r})\boldsymbol{u}(\boldsymbol{r})\rangle$. By virtue of the symmetry of our channel flow and the initial spectral distribution, these tensors are not spatially independent, but depend on y. The off-diagonal elements must vanish and $b_{33}(y)$ must be equal to $b_{11}(y)$. In figure 3(a), the dependence of the diagonal elements on y at time $t = 0.92$ is presented. One sees that our isotropic choice of the initial energy spectrum yields a nearly null anisotropy tensor at this time. In figure 3(b), we present this tensor at $t = 12.0$. Notice that the presence of the boundaries has caused the anisotropy of the velocity autocorrelation to become significant. Indeed, it is noteworthy that even at $y = 12.5$, the midplane, there is an anisotropy.

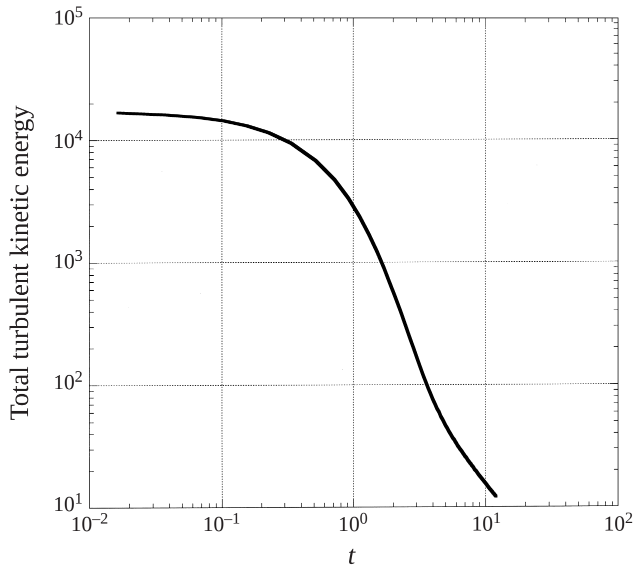

FIGURE 5. Total turbulent kinetic energy as a function of time.

In figure 4, we display the associated mean pressure profiles.

During this period, the total turbulent kinetic energy has been decaying as shown in figure 5.

3.6. *Summary of channel flow results*

We have analysed turbulent incompressible Navier–Stokes fluids confined by two parallel planar boundaries. Employing a Helmholtz decomposition, we derived a set of orthonormal solenoidal basis vectors presumably complete with respect to free-slip (i.e. stress-free) boundary conditions. The states of this basis, labelled solely by their wave vectors, were seen to be formed from linear superpositions of states of opposite helicity. Use of these states constitutes a very concise method of describing the slab of Navier–Stokes fluid. Unlike the case of a homogeneous fluid, the inhomogeneous free-slip case was seen not to admit basis states of specified helicity.

Introducing an intuitively plausible assumption that the ensemble-averaged values of the product of two different modes are uncorrelated (the RPA, (3.23)), which implied an absence of any net kinetic helicity in the velocity fluctuations, we derived an EDQNM evolution equation, (3.33), for an arbitrary energy spectrum that is initially invariant under reflection in a plane parallel to the boundaries of the fluid slab. We commented that if such a spectrum were an equipartition spectrum, it would be in equilibrium in the inviscid limit. Furthermore, we commented additionally that (*a*) the reflection-invariance would be propagated in time by the EDQNM equation, (*b*) the energy spectrum would be realizable, and (*c*) the form of the EDQNM equation, (3.33), can be collapsed to the form of (3.39). The evolution equation, (3.39), was shown to be strikingly analogous to that of homogeneous parity-invariant isotropic turbulence. Indeed we have seen that if the energy spectrum is isotropic in wave-vector space, the EDQNM evolution of the spectrum for the case of free-slip channel flow is nearly identical with that of homogeneous isotropic mirror-symmetric turbulence, even though the mapping from wave-vector space back to physical coordinate space will be neither homogeneous nor isotropic! At the same time, we observed that the evolution equation, (3.39), also possesses a noteworthy two-dimensional-like aspect as a result of the global geometry. We also presented the spectral components of the associated velocity autocorrelation with its structural vestiges of the velocity autocorrelation for an isotropic, homogeneous turbulence. Finally we presented numerical results showing the decay of turbulent kinetic energy during the development of anisotropy that was depicted at two times as a function of distance from the boundaries in a velocity autocorrelation that started nearly isotropic. The associated mean pressure profiles at those times were also shown.

The validity of our RPA in the absence of mean flows has recently received striking confirmation using an ensemble of direct numerical simulations (Ulitsky *et al.* 1999; Turner & Turner 2000).

The relationship of (3.39) to those equations that describe the evolution of two- and three-dimensional homogeneous isotropic turbulence suggests that further investigation of its properties both analytically and numerically will be fruitful for gleaning insight into the physics of inhomogeneous turbulence. For example, our equations can be utilized to study the effect of pressure–velocity and triple-velocity correlations on the development of the anisotropy observed in our numerical calculations. We have already made a start in this direction (Turner 1999).

The presence of a wave-vector-dependence of the energy spectrum promises that the study of the spectral transfers should be both intricate and rewarding. The extension of these techniques and ideas to other geometries provides a still further challenging problem.

Because we have restricted our analysis to only turbulent energy spectra that are reflection-invariant with respect to a plane parallel to the slab boundaries, we have been able to analyse only turbulent evolution in which there is no non-trivial mean flow. However, by relaxing this restriction, we are able to treat more general cases with our formalism. In a parallel manuscript, we have shown that when this restriction is lifted, a non-trivial mean flow can evolve out of the turbulence, even when no mean flow is present initially (Turner 1999). For the generation of a non-trivial mean flow (namely, a y-dependent flow) in the x-direction, we must have a spectrum in which, additionally, $U(\boldsymbol{k}, t)$ is not invariant under $k_z \to -k_z$. Similarly, for a mean flow to arise in the z-direction, the energy spectrum must not be invariant under $k_x \to -k_x$. The presence of such mean flows, in turn, affects the evolution of the turbulent spectrum. By virtue of the lower symmetry of the associated energy spectra, numerical computations with mean flows require more storage and time for their execution. Note, of course, that such non-trivial mean flows cannot occur in dynamics suffused by the assumption of statistical homogeneity.

We shall conclude this section of the manuscript by noting that Lesieur (1990*b*) had already remarked in 1989 that “Two-point closures were an invaluable tool to understand the phenomenology of isotropic turbulence … I do not think they can be much improved in this case. But they are also valid in anisotropic or inhomogeneous situations, although quite heavy to handle in these cases.” This heaviness has been alleviated by the methods of this manuscript as we shall continue to demonstrate in the remaining sections.

4. Results from other closures

4.1. *Introduction*

We have seen that obtaining the structure function for the Navier–Stokes equation is the starting point of developing a closure for the Navier–Stokes equation. For homogeneous turbulence, the translational symmetry permits a far more benign treatment than would otherwise be necessary for obtaining the EDQNM closure. For the case of inhomogeneous turbulence of a channel formed between two free-slip parallel boundaries, we have seen that the RPA permits a similarly benign development for the EDQNM closure.

This structure function was defined using a Helmholtz decomposition of the velocity field. At the nub of such decompositions is a helicity basis which obviates the cumbersome use of solenoidal projection operators. We shall demonstrate that the evolution equations of two other standard closures, the direct-interaction approximation (DIA) and the test-field model (TFM), used to describe three-dimensional homogeneous turbulence, can be specified in terms of the structure function. We shall extract the evolution equations of the two closures for two-dimensional incompressible homogeneous turbulence directly from the three-dimensional case. Analogous results for the inhomogeneous free-slip channel turbulence will also be shown using the RPA. As in § 3.4, we shall note the close resemblance of certain aspects of the evolution equations for the free-slip channel with corresponding aspects of the homogeneous turbulence cases.

The DIA and TFM provide especially interesting models of Navier–Stokes turbulence. The DIA describes the evolution of a two-time energy spectrum and does so with a closure both on the Navier–Stokes equation and on the equation describing the evolution of an associated Green's function. It is a fully self-consistent analytical turbulence theory. Computations with it are difficult, and it fails to satisfy Galilean invariance, a consequence of which is its inability to yield the anticipated Kolmogorov $k^{-5/3}$-behaviour of the homogeneous isotropic energy spectrum in the inertial range. The TFM, being a single-time model for the evolution of the energy spectrum, leads to somewhat more tractable computations. It is similar to the EDQNM model, but is more fundamental in that the eddy-damping functions are themselves determined by the TFM's equations. For details of the following analysis, see Turner (1997).

4.2. *The direction-interaction approximation*

4.2.1. *Three-dimensional homogeneous turbulence*

We return to the notation of § 2 and define $\tilde{g}_{ilm}(\boldsymbol{k},\boldsymbol{p},\boldsymbol{q})$ by

$$g_{ilm}(\boldsymbol{k},\boldsymbol{p},\boldsymbol{q}) \equiv \tilde{g}_{ilm}(\boldsymbol{k},\boldsymbol{p},\boldsymbol{q})\delta^{(3)}(\boldsymbol{k}+\boldsymbol{p}+\boldsymbol{q}). \tag{4.1}$$

The turbulent spectral tensor, $U_{ij}(\boldsymbol{k},t,t')$, is defined using the translational symmetry property of homogeneous turbulence,

$$\langle c_i(\boldsymbol{k},t)c_j(\boldsymbol{k}',t')\rangle \equiv U_{ij}(\boldsymbol{k},t,t')\delta^{(3)}(\boldsymbol{k}+\boldsymbol{k}'). \tag{4.2}$$

Using (2.22) and (4.2), we find the following symmetry properties of this spectral tensor:

$$U_{ij}(\boldsymbol{k},t,t') = U_{ji}(-\boldsymbol{k},t,t') = U^*_{ij}(-\boldsymbol{k},t,t'). \tag{4.3}$$

Thus fortified, one can derive readily the coupled equations that govern the evolution of the spectral tensor in the direct-interaction approximation:

$$\begin{aligned}\eta_{il}(\boldsymbol{k},t,s) = -4 \sum_{l',m',m,n=\pm} \int_{\boldsymbol{p}=\boldsymbol{k}-\boldsymbol{q}} \mathrm{d}^3 q\, G_{mn}(\boldsymbol{q},t,s) \\ \times U_{l'm'}(\boldsymbol{p},t,s)\tilde{g}^*_{m'ln}(\boldsymbol{p},-\boldsymbol{k},\boldsymbol{q})\tilde{g}_{ml'i}(\boldsymbol{q},\boldsymbol{p},-\boldsymbol{k}),\end{aligned} \tag{4.4}$$

$$\left(\frac{\partial}{\partial t}+\nu k^2\right)U_{ij}(\boldsymbol{k},t,t')+\sum_{l=\pm}\int_0^t \mathrm{d}s\,\eta_{il}(\boldsymbol{k},t,s)U_{lj}(\boldsymbol{k},s,t')$$
$$=2\sum_{l,m,l',m',n=\pm}\int_{\boldsymbol{p}=\boldsymbol{k}-\boldsymbol{q}}\mathrm{d}^3q\,\tilde{g}^*_{m'l'n}(\boldsymbol{q},\boldsymbol{p},-\boldsymbol{k})\tilde{g}_{mli}(\boldsymbol{q},\boldsymbol{p},-\boldsymbol{k})$$
$$\times\int_0^{t'}\mathrm{d}s\,G_{jn}(-\boldsymbol{k},t',s)U_{ll'}(\boldsymbol{p},t,s)U_{mm'}(\boldsymbol{q},t,s), \tag{4.5}$$

$$\left(\frac{\partial}{\partial t}+\nu k^2\right)G_{ij}(\boldsymbol{k},t,t')+\sum_{l=\pm}\int_{t'}^t \mathrm{d}s\,\eta_{il}(\boldsymbol{k},t,s)G_{lj}(\boldsymbol{k},s,t')=\delta_{ij}\delta(t-t'), \tag{4.6}$$

where the Green's function, $G_{ij}(\boldsymbol{k},t,t')$ satisfies the following conditions:

$$G_{ij}(\boldsymbol{k},t+0^+,t)=\delta_{ij},\qquad G_{ij}(\boldsymbol{k},t,t')=0,\quad t<t'. \tag{4.7}$$

Equations (4.4)–(4.7) constitute the DIA equations that describe the evolution of the spectral tensor for a completely arbitrary incompressible statistically homogeneous Navier–Stokes fluid turbulence, a turbulence that need not be statistically either isotropic or mirror-symmetric. One may verify that these equations reduce to the well-known DIA equations for the special case when the turbulence is both statistically isotropic and mirror-symmetric (Turner 1997).

4.2.2. *Two-dimensional homogeneous turbulence*

We shall demonstrate here how one can obtain directly the equations of the two-dimensional DIA closure from those of the three-dimensional closure. The velocity is taken to be in only the $\hat{\boldsymbol{x}}$- and $\hat{\boldsymbol{y}}$-directions, and the z-coordinate is taken to be ignorable. Therefore, we choose as our solenoidal basis vectors, the vectors

$$\boldsymbol{\sigma}_{(2)}(\boldsymbol{k},\boldsymbol{r})\equiv\frac{\boldsymbol{\xi}_+(\boldsymbol{k},\boldsymbol{r})+\boldsymbol{\xi}_-(\boldsymbol{k},\boldsymbol{r})}{\sqrt{2}}=\boldsymbol{\sigma}^*_{(2)}(-\boldsymbol{k},\boldsymbol{r}). \tag{4.8}$$

These vectors have no z-component. We are using the subscript (2) to distinguish these functions of two-dimensional homogenous turbulence from those of channel flow. These functions provide a complete orthonormal set when the integral is taken over the (x,y)-plane, so that we can expand the velocity as

$$\boldsymbol{u}(\boldsymbol{r},t)=\int\mathrm{d}^2k\,c(\boldsymbol{k},t)\boldsymbol{\sigma}_{(2)}(\boldsymbol{k},\boldsymbol{r}), \tag{4.9}$$

in the absence of a mean flow, a flow which can be trivially Galilean-transformed away when present. We observe that

$$\nabla\times\boldsymbol{\sigma}_{(2)}(\boldsymbol{k},\boldsymbol{r})=k\boldsymbol{\Delta}_{(2)}(\boldsymbol{k},\boldsymbol{r}),\qquad\nabla\times\boldsymbol{\Delta}_{(2)}(\boldsymbol{k},\boldsymbol{r})=k\boldsymbol{\sigma}_{(2)}(\boldsymbol{k},\boldsymbol{r}), \tag{4.10}$$

where also

$$\frac{1}{(2\pi)^2}\int\mathrm{d}^2r\boldsymbol{\sigma}_{(2)}(\boldsymbol{k},\boldsymbol{r})\cdot\boldsymbol{\sigma}^*_{(2)}(\boldsymbol{k}',\boldsymbol{r})=\frac{1}{(2\pi)^2}\int\mathrm{d}^2r\,\boldsymbol{\Delta}_{(2)}(\boldsymbol{k},\boldsymbol{r})\cdot\boldsymbol{\Delta}^*_{(2)}(\boldsymbol{k}',\boldsymbol{r})$$
$$=\delta^{(2)}(\boldsymbol{k}-\boldsymbol{k}'), \tag{4.11}$$

$$\boldsymbol{\omega}(\boldsymbol{r},t)=\int\mathrm{d}^2k\,kc(\boldsymbol{k},t)\boldsymbol{\Delta}_{(2)}(\boldsymbol{k},\boldsymbol{r}). \tag{4.12}$$

One observes that

$$\Delta_{(2)}(\boldsymbol{k},\boldsymbol{r}) \equiv \frac{\xi_+(\boldsymbol{k},\boldsymbol{r}) - \xi_-(\boldsymbol{k},\boldsymbol{r})}{\sqrt{2}} = \Delta^*_{(2)}(-\boldsymbol{k},\boldsymbol{r}). \tag{4.13}$$

As in the case of three-dimensional DIA, we define the spectral density, $U(\boldsymbol{k},t,t')$, using the assumption of statistical homogeneity of the turbulence, as

$$\langle c(\boldsymbol{k},t,)c^*(\boldsymbol{k}',t')\rangle \equiv \delta^{(2)}(\boldsymbol{k}-\boldsymbol{k}')U(\boldsymbol{k},t,t'), \tag{4.14}$$

in which U again satisfies the symmetry properties of (4.3). The fluid's kinetic energy can be expressed as

$$\frac{\langle u^2(\boldsymbol{r},t)\rangle}{2} = \frac{1}{2}\int \mathrm{d}^2k\, U(\boldsymbol{k},t,t). \tag{4.15}$$

Using the general evolution equations, (2.19) and (2.20), but observing that (4.8) and (4.9) imply that $c_{\pm}(\boldsymbol{k},t) = c(\boldsymbol{k},t)/\sqrt{2}$, we find that the evolution equation for the spectral coefficients for the degenerate case of two-dimensional turbulence can be written as

$$\left(\frac{\partial}{\partial t} + \nu k^2\right) c(\boldsymbol{k},t) = \int \mathrm{d}^2q\, \mathrm{d}^2p\, g_{(2)}(\boldsymbol{p},\boldsymbol{q},-\boldsymbol{k})c(\boldsymbol{p},t)c(\boldsymbol{q},t), \tag{4.16}$$

where the structure function, $g_{(2)}$ can be expressed as

$$g_{(2)}(\boldsymbol{p},\boldsymbol{q},\boldsymbol{k}) = \frac{1}{\sqrt{2}}\sum_{l,m=\pm} g_{lmi}(\boldsymbol{p},\boldsymbol{q},\boldsymbol{k}) \tag{4.17}$$

with

$$g_{lmi}(\boldsymbol{p},\boldsymbol{q},\boldsymbol{k}) = \delta^{(2)}(\boldsymbol{k}+\boldsymbol{p}+\boldsymbol{q})\tilde{g}_{lmi}(\boldsymbol{p},\boldsymbol{q},\boldsymbol{k}). \tag{4.18}$$

We thus see from (2.18) and (2.20) that $\tilde{g}_{lmi}(\boldsymbol{p},\boldsymbol{q},\boldsymbol{k})$ is given by

$$\begin{aligned}\tilde{g}_{lmi}(\boldsymbol{p},\boldsymbol{q},\boldsymbol{k}) = &-\frac{\mathrm{i}s_i s_l s_m}{2^{3/2}}\left[\frac{A(k,p,q)}{kpq}\right] \\ &\times \exp\left[\mathrm{i}(s_i\phi_{\boldsymbol{k}} + s_l\phi_{\boldsymbol{p}} + s_m\phi_{\boldsymbol{q}})_{\hat{\boldsymbol{n}}(\boldsymbol{k},\boldsymbol{p},\boldsymbol{q})}\right](s_m q - s_l p)(s_i k + s_l p + s_m q).\end{aligned} \tag{4.19}$$

Because the wave vectors are orthogonal to the z-direction, (2.2), (2.12), and (2.13) imply that

$$\sin(\phi_{\boldsymbol{k}})_{\hat{\boldsymbol{n}}(\boldsymbol{p},\boldsymbol{q},\boldsymbol{k})} = \sin(\phi_{\boldsymbol{p}})_{\hat{\boldsymbol{n}}(\boldsymbol{p},\boldsymbol{q},\boldsymbol{k})} = \sin(\phi_{\boldsymbol{q}})_{\hat{\boldsymbol{n}}(\boldsymbol{p},\boldsymbol{q},\boldsymbol{k})} = \pm 1 \equiv s_H(\boldsymbol{k},\boldsymbol{p},\boldsymbol{q}), \tag{4.20}$$

in which the upper sign is chosen when $\hat{\boldsymbol{n}}(\boldsymbol{p},\boldsymbol{q},\boldsymbol{k})$ points along the $+\hat{\boldsymbol{z}}$-direction, and the lower sign when $\hat{\boldsymbol{n}}(\boldsymbol{p},\boldsymbol{q},\boldsymbol{k})$ points along the $-\hat{\boldsymbol{z}}$-direction. This defines the new variable $s_H(\boldsymbol{k},\boldsymbol{p},\boldsymbol{q})$. Observe that s_H changes sign under interchange of any two of its wave-vector arguments and also that $s_H(\boldsymbol{k},\boldsymbol{p},\boldsymbol{q}) = s_H(-\boldsymbol{k},-\boldsymbol{p},-\boldsymbol{q})$. Using these properties, we find that

$$g_{(2)}(\boldsymbol{p},\boldsymbol{q},\boldsymbol{k}) = \delta^{(2)}(\boldsymbol{p}+\boldsymbol{q}+\boldsymbol{k})\tilde{g}_{(2)}(\boldsymbol{p},\boldsymbol{q},\boldsymbol{k}), \tag{4.21}$$

with

$$\tilde{g}_{(2)}(\boldsymbol{p},\boldsymbol{q},\boldsymbol{k}) = -s_H(\boldsymbol{k},\boldsymbol{p},\boldsymbol{q})\left[\frac{A(k,p,q)}{kpq}\right](q^2 - p^2). \tag{4.22}$$

Using this reduction of the three-dimensional representation to the two-dimensional representation, we immediately can write down the DIA equations for an arbitrary two-dimensional statistically homogeneous turbulence:

$$\eta(\boldsymbol{k},t,s) = -4\int_{\boldsymbol{q}=\boldsymbol{k}-\boldsymbol{p}} \mathrm{d}^2p\, G(\boldsymbol{q},t,s)U(\boldsymbol{p},t,s)\tilde{g}_{(2)}(\boldsymbol{p},\boldsymbol{q},-\boldsymbol{k})\tilde{g}_{(2)}(-\boldsymbol{p},\boldsymbol{k},-\boldsymbol{q})$$
$$= 4\int_{\boldsymbol{q}=\boldsymbol{k}-\boldsymbol{p}} \mathrm{d}^2p \frac{A^2(k,p,q)}{k^2p^2q^2}(q^2-p^2)(k^2-p^2)G(\boldsymbol{q},t,s)U(\boldsymbol{p},t,s), \tag{4.23}$$

$$\left(\frac{\partial}{\partial t} + \nu k^2\right) U(\boldsymbol{k},t,t') + \int_0^t \mathrm{d}s\, \eta(\boldsymbol{k},t,s)U(\boldsymbol{k},s,t')$$
$$= -4\int_{\boldsymbol{q}=\boldsymbol{k}-\boldsymbol{p}} \mathrm{d}^2p\, \tilde{g}_{(2)}(\boldsymbol{p},\boldsymbol{q},-\boldsymbol{k})\tilde{g}_{(2)}(-\boldsymbol{p},\boldsymbol{k},-\boldsymbol{q}) \int_0^{t'} \mathrm{d}s\, G(-\boldsymbol{k},t',s)U(\boldsymbol{q},t,s)U(\boldsymbol{p},t,s)$$
$$= 2\int_{\boldsymbol{q}=\boldsymbol{k}-\boldsymbol{p}} \mathrm{d}^2p|\tilde{g}_{(2)}(\boldsymbol{p},\boldsymbol{q},-\boldsymbol{k})|^2 \int_0^{t'} \mathrm{d}s\, G(-\boldsymbol{k},t',s)U(\boldsymbol{q},t,s)U(\boldsymbol{p},t,s)$$
$$= 4\int_{\boldsymbol{q}=\boldsymbol{k}-\boldsymbol{p}} \mathrm{d}^2p \frac{A^2(k,p,q)}{k^2p^2q^2}(q^2-p^2)(k^2-p^2) \int_0^{t'} \mathrm{d}s\, G(-\boldsymbol{k},t',s)U(\boldsymbol{q},t,s)U(\boldsymbol{p},t,s)$$
$$= 2\int_{\boldsymbol{q}=\boldsymbol{k}-\boldsymbol{p}} \mathrm{d}^2p \frac{A^2(k,p,q)}{k^2p^2q^2}(q^2-p^2)^2 \int_0^{t'} \mathrm{d}s\, G(-\boldsymbol{k},t',s)U(\boldsymbol{q},t,s)U(\boldsymbol{p},t,s), \tag{4.24}$$

$$\left(\frac{\partial}{\partial t} + \nu k^2\right) G(\boldsymbol{k},t,t') + \int_{t'}^t \mathrm{d}s\, \eta(\boldsymbol{k},t,s)G(\boldsymbol{k},s,t') = \delta(t-t'). \tag{4.25}$$

Again the spectrum is defined by

$$\langle c(\boldsymbol{k},t)c^*(\boldsymbol{k}',t')\rangle \equiv \delta^{(2)}(\boldsymbol{k}-\boldsymbol{k}')U(\boldsymbol{k},t,t') \tag{4.26}$$

and the Green's function $G(\boldsymbol{k},t,t')$ satisfies

$$G(\boldsymbol{k},t+0^+,t) = 1, \qquad G(\boldsymbol{k},t,t') = 0, \quad t < t'. \tag{4.27}$$

These equations reduce to the standard DIA equations for the case of two-dimensional *isotropic* turbulence (Turner 1997).

4.2.3. *Three-dimensional free-slip channel flow*

We again represent the turbulent flow described in § 3 using the set of solenoidal basis vectors employed there. The structure function, $g(\boldsymbol{k},\boldsymbol{p},\boldsymbol{q})$, is that given in (3.21). We again call upon the RPA to define the spectrum, $U(\boldsymbol{k},t,t')$, by

$$\langle c(\boldsymbol{k},t)c(\boldsymbol{k}',t')\rangle = \delta_{\boldsymbol{k}+\boldsymbol{k}',\boldsymbol{0}}U(\boldsymbol{k},t,t'). \tag{4.28}$$

In analogy with (4.3), one readily notes that

$$U(\boldsymbol{k},t,t') = U(-\boldsymbol{k},t',t) = U^*(-\boldsymbol{k},t,t'). \tag{4.29}$$

To make contact with the physical energy spectrum when $t \to t'$, we observe that

$$\frac{1}{2L_xL_yL_z}\int \mathrm{d}^3r\, u^2(\boldsymbol{r},t) = \sum_{\boldsymbol{k}} \frac{U(\boldsymbol{k},t,t)}{4}. \tag{4.30}$$

in the absence of a net flux. We therefore define $U_E(\boldsymbol{k},t,t') \equiv U(\boldsymbol{k},t,t')/2$. One can derive the DIA for this case to find

$$\eta(\boldsymbol{k},t,s) = -8\sum_{\boldsymbol{q},\boldsymbol{p}} G(\boldsymbol{q},t,s)U_E(\boldsymbol{p},t,s)g(\boldsymbol{p},\boldsymbol{q},-\boldsymbol{k})g^*(-\boldsymbol{k},\boldsymbol{p},\boldsymbol{q}), \tag{4.31}$$

$$\left(\frac{\partial}{\partial t}+\nu k^2\right)U_E(\boldsymbol{k},t,t')+\int_0^t \mathrm{d}s\,\eta(\boldsymbol{k},t,s)U_E(\boldsymbol{k},s,t')$$
$$=4\sum_{\boldsymbol{q},\boldsymbol{p}}|g(\boldsymbol{q},\boldsymbol{p},-\boldsymbol{k})|^2\int_0^{t'}\mathrm{d}s\,G(-\boldsymbol{k},t',s)U_E(\boldsymbol{q},t,s)U_E(\boldsymbol{p},t,s), \tag{4.32}$$

$$\left(\frac{\partial}{\partial t}+\nu k^2\right)G(\boldsymbol{k},t,t')+\int_{t'}^t \mathrm{d}s\,\eta(\boldsymbol{k},t,s)G(\boldsymbol{k},s,t')=\delta(t-t'). \tag{4.33}$$

Again the Green's function, $G(\boldsymbol{k},t,t')$ satisfies

$$G(\boldsymbol{k},t+0^+,t)=1, \qquad G(\boldsymbol{k},t,t')=0, \quad t<t'. \tag{4.34}$$

We are assuming the symmetry under reflection of the y-component of the wave vectors,

$$\eta(\boldsymbol{k},t,s)=\eta(\boldsymbol{k}_-,t,s), \quad U_E(\boldsymbol{k},t,s)=U_E(\boldsymbol{k}_-,t,s), \quad G(\boldsymbol{k},t,s)=G(\boldsymbol{k}_-,t,s). \tag{4.35}$$

This symmetry is maintained by the DIA evolution equations, (4.31)–(4.33). One can re-express these equations still further using the formula for the structure functions, (3.21):

$$\begin{aligned}
&\eta(\boldsymbol{k},t,s)\\
&\quad=\frac{1}{4k^2}\sum_{\boldsymbol{p},\boldsymbol{q}\ni p_yq_y\neq 0}\delta_{\boldsymbol{q}+\boldsymbol{p},\boldsymbol{k}}\sin^2(\alpha_{\boldsymbol{k}})[(p^2-q^2)(k^2-q^2)+k^2p^2]G(\boldsymbol{p},t,s)U_E(\boldsymbol{q},t,s)\\
&\quad+\frac{\delta_{k_y,0}}{k^2}\sum_{\boldsymbol{p},\boldsymbol{q}\ni p_y=q_y=0}\delta_{k_x,p_x+q_x}\delta_{k_z,p_z+q_z}\sin^2(\alpha_{\boldsymbol{k}})[(k^2-p^2)(q^2-p^2)]G(\boldsymbol{q},t,s)U_E(\boldsymbol{p},t,s)\\
&\quad+\text{hybrid contributions,}
\end{aligned} \tag{4.36}$$

$$\begin{aligned}
&\left(\frac{\partial}{\partial t}+\nu k^2\right)U_E(\boldsymbol{k},t,t')+\int_0^t \mathrm{d}s\,\eta(\boldsymbol{k},t,s)U_E(\boldsymbol{k},s,t')\\
&\quad=\frac{1}{4k^2}\sum_{\boldsymbol{p},\boldsymbol{q}\ni p_yq_y\neq 0}\delta_{\boldsymbol{q}+\boldsymbol{p},\boldsymbol{k}}\sin^2(\alpha_{\boldsymbol{k}})[(p^2-q^2)(k^2-q^2)+k^2p^2]\\
&\qquad\qquad\times\int_0^{t'}\mathrm{d}s\,G(\boldsymbol{k},t',s)U_E(\boldsymbol{q},t,s)U_E(\boldsymbol{p},t,s)\\
&\quad+\frac{\delta_{k_y,0}}{k^2}\sum_{\boldsymbol{p},\boldsymbol{q}\ni p_y=q_y=0}\delta_{q_x+p_x,k_x}\delta_{q_z+p_z,k_z}\sin^2(\alpha_{\boldsymbol{k}})[(k^2-p^2)(q^2-p^2)]\\
&\qquad\qquad\times\int_0^{t'}\mathrm{d}s\,G(\boldsymbol{k},t',s)U_E(\boldsymbol{q},t,s)U_E(\boldsymbol{p},t,s)\\
&\quad+\text{hybrid contributions,}
\end{aligned} \tag{4.37}$$

$$\left(\frac{\partial}{\partial t}+\nu k^2\right)G(\boldsymbol{k},t,t')+\int_t^{t'} \mathrm{d}s\,\eta(\boldsymbol{k},t,s)G(\boldsymbol{k},s,t')=\delta(t-t'), \tag{4.38}$$

where again $G(\boldsymbol{k},t,t')$ satisfies (4.34).

4.3. *The test-field model*

4.3.1. *Introduction*

Unlike the DIA closure, the test-field model (TFM) closure constitutes a single-time closure for the spectral density, U. The TFM method (Leith & Kraichnan 1972) of closing the second-order moment equations to derive the time-evolution equation of U requires two more structure functions that have no relevance to the spectral representation of the Navier–Stokes equation itself. Indeed, we distill these structure functions from the TFM prescription of focusing on the time-evolution of a test-field's solenoidal component, $\boldsymbol{v}^s(\boldsymbol{r},t)$, due to spatial gradients of its irrotational component along the fluid velocity, $\boldsymbol{u}(\boldsymbol{r},t)$, and on the time-evolution of the test-field's irrotational component, $\boldsymbol{v}^c(\boldsymbol{r},t)$, due to spatial gradients of its solenoidal component along the fluid velocity, where the test-field's velocity $\boldsymbol{v}$ is the sum of $\boldsymbol{v}^s+\boldsymbol{v}^c$. This passive convection scheme ignores any pressure field.

The derivation of the TFM equations is rather laborious. We have followed the procedure detailed in Turner (1997) using the appropriate solenoidal basis vectors already given in the above sections for representing the velocity field. However, for the TFM, we also need to represent an irrotational velocity field, $\boldsymbol{v}^c(\boldsymbol{r},t)$, for each of the three geometries: three-dimensional homogeneous, two-dimensional homogeneous, and the channel flow between two parallel infinite free-slip boundaries. These representations and the orthogonality properties of the new functions are given by:

three ($n=3$) *and two-dimensional* ($n=2$, $k_z=0$) *homogeneous geometry*

$$\boldsymbol{v}^c(\boldsymbol{r},t)=\sum_{i=\pm}\int \mathrm{d}^n k\,\tilde{d}_i(\boldsymbol{k},t)\nabla\Psi(\boldsymbol{k},\boldsymbol{r}),\qquad \Psi(\boldsymbol{k},\boldsymbol{r})=\frac{\exp(\mathrm{i}\boldsymbol{k}\cdot\boldsymbol{r})}{k},\tag{4.39}$$

$$\frac{1}{(2\pi)^n}\int \mathrm{d}^n r\,\nabla\Psi^*(\boldsymbol{k},\boldsymbol{r})\cdot\nabla\Psi(\boldsymbol{k}',\boldsymbol{r})=\delta^{(n)}(\boldsymbol{k}-\boldsymbol{k}'),\tag{4.40}$$

$$\int \mathrm{d}^n r\,\nabla\Psi^*(\boldsymbol{k},\boldsymbol{r})\cdot\xi_\pm(\boldsymbol{k}',\boldsymbol{r})=\int \mathrm{d}^n r\,\nabla\cdot[\Psi^*(\boldsymbol{k},\boldsymbol{r})\xi_\pm(\boldsymbol{k}',\boldsymbol{r})]=0;\tag{4.41}$$

three-dimensional free-slip channel flow

$$\begin{gathered}\boldsymbol{v}^c(\boldsymbol{r},t)=\textstyle\sum_{k\ni m\geqslant 0}\tilde{d}(\boldsymbol{k},t)\boldsymbol{\kappa}(\boldsymbol{k},\boldsymbol{r}),\\ \boldsymbol{\kappa}(\boldsymbol{k},\boldsymbol{r})=\dfrac{\epsilon_m}{2k}\sum_{s=\pm}\mathrm{i}\boldsymbol{k}_s\exp(\mathrm{i}\boldsymbol{k}_s\cdot\boldsymbol{r}),\quad \varepsilon_m\equiv\begin{cases}1, & m\neq 0\\ 1/\sqrt{2}, & m=0,\end{cases}\end{gathered}\tag{4.42}$$

$$\frac{2}{L_xL_yL_z}\int \mathrm{d}^3 r\,\boldsymbol{\kappa}^*(\boldsymbol{k},\boldsymbol{r})\cdot\boldsymbol{\kappa}(\boldsymbol{k}',\boldsymbol{r})=\delta_{\boldsymbol{k},\boldsymbol{k}'},\tag{4.43}$$

$$\frac{2}{L_xL_yL_z}\int \mathrm{d}^3 r\,\boldsymbol{\kappa}^*(\boldsymbol{k},\boldsymbol{r})\cdot\boldsymbol{\Delta}(\boldsymbol{k}',\boldsymbol{r})=0.\tag{4.44}$$

The reader who is interested in further details of the derivation of the final TFM equations for the three geometries under consideration should consult Turner (1997). Space limitations of this manuscript restrict us merely to listing the final TFM equations for each of the geometries.

4.3.2. *Three-dimensional homogeneous isotropic reflection-invariant turbulence results*

The fluid velocity is given by

$$\boldsymbol{u}(\boldsymbol{r},t)=\sum_{i=\pm}\int \mathrm{d}^3k\, c_{s_i}(\boldsymbol{k},t)\boldsymbol{\xi}_{s_i}(\boldsymbol{k},\boldsymbol{r}). \tag{4.45}$$

We are restricting our considerations here only to the case where the fluid turbulence is statistically homogeneous, isotropic, and reflection-invariant. The energy spectrum $U_E(k,t)$ is then defined by

$$\langle c_i(\boldsymbol{k},t)c_j^*(\boldsymbol{k}',t)\rangle=\delta_{ij}\delta^{(3)}(\boldsymbol{k}-\boldsymbol{k}')\frac{U_E(k,t)}{2}. \tag{4.46}$$

The TFM evolution of this spectrum is then given by

$$\left(\frac{\partial}{\partial t}+2\nu k^2\right)U_E(k,t)=\frac{\pi}{k^3}\int_{\boldsymbol{p}+\boldsymbol{q}+\boldsymbol{k}=\boldsymbol{0}}\mathrm{d}q\,\mathrm{d}p\,qp\sin^2(\alpha_{\boldsymbol{k}})\theta(p,q,k;t)$$
$$\times[U_E(q,t)-U_E(k,t)]U_E(p,t)[(k^2-p^2)(q^2-p^2)+k^2q^2]. \tag{4.47}$$

Recall from §2.1 that $\alpha_{\boldsymbol{k}}$ is the angle of the kpq-triangle opposite the side having magnitude k. To determine the function $\theta(k,p,q;t)$, we use the following equations of the TFM for θ and $\tilde{\theta}$:

$$\left[\frac{\partial}{\partial t}+\nu(k^2+p^2+q^2)\right]\theta(k,p,q;t)=1-[\mu^s(k,t)+\mu^s(p,t)+\mu^s(q,t)]\theta(k,p,q;t), \tag{4.48}$$

$$\left[\frac{\partial}{\partial t}+\nu(k^2+p^2+q^2)\right]\tilde{\theta}(k,p,q;t)=1-[\mu^s(k,t)+\mu^s(p,t)+\mu^c(q,t)]\tilde{\theta}(k,p,q;t), \tag{4.49}$$

along with the initial conditions

$$\theta(k,p,q;0)=\tilde{\theta}(k,p,q;0)=0. \tag{4.50}$$

The damping factors, μ^s and μ^c are then defined in terms of the $\tilde{\theta}$ and the energy spectrum:

$$\mu^s(k,t)\equiv\frac{\pi}{2}\int_{\boldsymbol{p}+\boldsymbol{q}+\boldsymbol{k}=\boldsymbol{0}}\mathrm{d}q\,\mathrm{d}p\left(\frac{qp}{k}\right)^3\sin^4(\alpha_{\boldsymbol{k}})\tilde{\theta}(p,k,q;t)U_E(p,t), \tag{4.51}$$

$$\mu^c(k,t)\equiv\pi\int_{\boldsymbol{p}+\boldsymbol{q}+\boldsymbol{k}=\boldsymbol{0}}\mathrm{d}q\,\mathrm{d}p\left(\frac{qp}{k}\right)^3\sin^4(\alpha_{\boldsymbol{k}})\tilde{\theta}(p,q,k;t)U_E(p,t). \tag{4.52}$$

4.3.3. *Two-dimensional homogeneous turbulence results*

The fluid velocity is given by

$$\boldsymbol{u}(\boldsymbol{r},t)=\int \mathrm{d}^2k\, c(\boldsymbol{k},t)\boldsymbol{\sigma}_{(2)}(\boldsymbol{k},\boldsymbol{r}). \tag{4.53}$$

The energy spectrum, $U(k,t)$, is defined by

$$\langle c(\boldsymbol{k},t)c^*(\boldsymbol{k}',t)\rangle\equiv\delta^{(2)}(\boldsymbol{k}-\boldsymbol{k}')U(\boldsymbol{k},t), \tag{4.54}$$

where $U(\boldsymbol{k},t)=U(-\boldsymbol{k},t)$. The TFM evolution of this spectrum is then given by

$$\left(\frac{\partial}{\partial t}+2\nu k^2\right)U(\boldsymbol{k},t)=-8\int \mathrm{d}^2p\,\mathrm{d}^2q\,\delta^{(2)}(\boldsymbol{p}+\boldsymbol{q}+\boldsymbol{k})\frac{A^2(k,p,q)}{k^2p^2q^2}$$
$$\times(q^2-p^2)(k^2-p^2)\{\theta(\boldsymbol{k},\boldsymbol{p},\boldsymbol{q},t)[U(\boldsymbol{k},t)-U(\boldsymbol{q},t)]U(\boldsymbol{p},t)\}. \tag{4.55}$$

The function, θ, is a totally symmetric function of its wave-vector arguments satisfying $\theta(\boldsymbol{k},\boldsymbol{p},\boldsymbol{q},t) = \theta^*(-\boldsymbol{k},-\boldsymbol{p},-\boldsymbol{q},t)$. We are choosing θ to be a real function, i.e. $\theta(\boldsymbol{k},\boldsymbol{p},\boldsymbol{q},t) = \theta^*(\boldsymbol{k},\boldsymbol{p},\boldsymbol{q},t)$. We shall also be utilizing a function $\tilde{\theta}$, a real function satisfying $\tilde{\theta}(\boldsymbol{k},\boldsymbol{p},\boldsymbol{q},t) = \tilde{\theta}^*(-\boldsymbol{k},-\boldsymbol{p},-\boldsymbol{q},t) = \tilde{\theta}^*(\boldsymbol{k},\boldsymbol{p},\boldsymbol{q},t)$. These functions are required to satisfy

$$\left[\frac{\partial}{\partial t} + \nu(k^2+p^2+q^2)\right]\theta(\boldsymbol{k},\boldsymbol{p},\boldsymbol{q};t) = 1 - [\mu^s_{(2)}(\boldsymbol{k},t) + \mu^s_{(2)}(\boldsymbol{p},t) + \mu^s_{(2)}(\boldsymbol{q},t)]\theta(\boldsymbol{k},\boldsymbol{p},\boldsymbol{q};t), \tag{4.56}$$

$$\left[\frac{\partial}{\partial t} + \nu(k^2+p^2+q^2)\right]\tilde{\theta}(\boldsymbol{k},\boldsymbol{p},\boldsymbol{q};t) = 1 - [\mu^s_{(2)}(\boldsymbol{k},t) + \mu^s_{(2)}(\boldsymbol{p},t) + \mu^c_{(2)}(\boldsymbol{q},t)]\tilde{\theta}(\boldsymbol{k},\boldsymbol{p},\boldsymbol{q};t), \tag{4.57}$$

with the initial conditions

$$\theta(\boldsymbol{k},\boldsymbol{p},\boldsymbol{q},0) = \tilde{\theta}(\boldsymbol{k},\boldsymbol{p},\boldsymbol{q},0) = 0. \tag{4.58}$$

The damping factors are defined by

$$\mu^s_{(2)}(\boldsymbol{k},t) = 16\int \mathrm{d}^2p\,\mathrm{d}^2q\,\delta^{(2)}(\boldsymbol{p}+\boldsymbol{q}+\boldsymbol{k})\frac{A^4(k,p,q)}{k^2p^2q^2}\tilde{\theta}(\boldsymbol{p},\boldsymbol{k},\boldsymbol{q},t)U(\boldsymbol{p},t), \tag{4.59}$$

$$\mu^c_{(2)}(\boldsymbol{k},t) = 16\int \mathrm{d}^2p\,\mathrm{d}^2q\,\delta^{(2)}(\boldsymbol{p}+\boldsymbol{q}+\boldsymbol{k})\frac{A^4(k,p,q)}{k^2p^2q^2}\tilde{\theta}(\boldsymbol{p},\boldsymbol{q},\boldsymbol{k},t)U(\boldsymbol{p},t). \tag{4.60}$$

For the case when this two-dimensional turbulence is isotropic these equations can be further simplified:

$$\begin{aligned}\left(\frac{\partial}{\partial t} + 2\nu k^2\right)U(k,t) = \frac{2}{k^2}\int_{\boldsymbol{q}+\boldsymbol{p}=\boldsymbol{k}} &\mathrm{d}p\,\mathrm{d}q\,\sin(\alpha_{\boldsymbol{k}})\theta(k,p,q;t)\\ &\times(q^2-p^2)(k^2-p^2)[U(q,t)-U(k,t)]U(p,t),\end{aligned} \tag{4.61}$$

$$\begin{aligned}&\left[\frac{\partial}{\partial t} + \nu(k^2+p^2+q^2)\right]\theta(k,p,q;t)\\ &\qquad = 1 - [\mu^s_{(2)}(k,t) + \mu^s_{(2)}(p,t) + \mu^s_{(2)}(q,t)]\theta(k,p,q;t),\end{aligned} \tag{4.62}$$

$$\begin{aligned}&\left[\frac{\partial}{\partial t} + \nu(k^2+p^2+q^2)\right]\tilde{\theta}(k,p,q;t)\\ &\qquad = 1 - [\mu^s_{(2)}(k,t) + \mu^s_{(2)}(p,t) + \mu^c_{(2)}(q,t)]\tilde{\theta}(k,p,q;t),\end{aligned} \tag{4.63}$$

$$\mu^s_{(2)}(k,t) = \frac{1}{k^2}\int_{\boldsymbol{q}+\boldsymbol{p}=\boldsymbol{k}}\mathrm{d}p\,\mathrm{d}q\,\sin^3(\alpha_{\boldsymbol{k}})\tilde{\theta}(p,k,q;t)p^2q^2U(p,t), \tag{4.64}$$

$$\mu^c_{(2)}(k,t) = \frac{1}{k^2}\int_{\boldsymbol{q}+\boldsymbol{p}=\boldsymbol{k}}\mathrm{d}p\,\mathrm{d}q\,\sin^3(\alpha_{\boldsymbol{k}})\tilde{\theta}(p,q,k;t)p^2q^2U(p,t), \tag{4.65}$$

in which θ and $\tilde{\theta}$ satisfy the initial conditions

$$\theta(k,p,q;0) = \tilde{\theta}(k,p,q,0) = 0. \tag{4.66}$$

4.3.4. *Three-dimensional free-slip channel flow results*

The fluid velocity is given by

$$\boldsymbol{u}(\boldsymbol{r},t) = \sum_{\boldsymbol{k}} c(\boldsymbol{k},t)\boldsymbol{\Delta}(\boldsymbol{k},\boldsymbol{r}). \tag{4.67}$$

The energy spectrum is defined by

$$\langle c(\boldsymbol{k},t)c^*(\boldsymbol{k}',t)\rangle \equiv 2U_E(\boldsymbol{k},t)\delta_{\boldsymbol{k},\boldsymbol{k}'}, \tag{4.68}$$

and is assumed to satisfy the symmetry condition

$$U_E(\boldsymbol{k},t) = U_E(\boldsymbol{k}_-,t), \tag{4.69}$$

a condition that is consistent at all times with the TFM evolution equations below. This condition is required for there to be no mean flow, as we have mentioned above in § 3.3. The TFM evolution of this spectrum is then given by

$$\begin{aligned}\left(\frac{\partial}{\partial t} + 2\nu k^2\right) U_E(\boldsymbol{k},t) \\ &= 8\sum_{\boldsymbol{p},\boldsymbol{q}}\{\theta(\boldsymbol{k},\boldsymbol{p},\boldsymbol{q},t)g(\boldsymbol{p},\boldsymbol{q},\boldsymbol{k})g(-\boldsymbol{p},-\boldsymbol{k},-\boldsymbol{q})[U_E(\boldsymbol{k},t) - U_E(\boldsymbol{q},t)]U_E(\boldsymbol{p},t)\} \\ &\quad +(\boldsymbol{k} \Leftrightarrow -\boldsymbol{k}),\end{aligned} \tag{4.70}$$

where $g(\boldsymbol{k},\boldsymbol{p},\boldsymbol{q})$ is defined by (3.21).

The function θ is a totally symmetric function of its wave-vector arguments satisfying $\theta(\boldsymbol{k},\boldsymbol{p},\boldsymbol{q},t) = \theta^*(-\boldsymbol{k},-\boldsymbol{p},-\boldsymbol{q},t)$. We are choosing θ to be a real function, i.e. $\theta(\boldsymbol{k},\boldsymbol{p},\boldsymbol{q},t) = \theta^*(\boldsymbol{k},\boldsymbol{p},\boldsymbol{q},t)$. We shall also be utilizing a function $\tilde{\theta}$, a real function satisfying $\tilde{\theta}(\boldsymbol{k},\boldsymbol{p},\boldsymbol{q},t) = \tilde{\theta}^*(-\boldsymbol{k},-\boldsymbol{p},-\boldsymbol{q},t) = \tilde{\theta}^*(\boldsymbol{k},\boldsymbol{p},\boldsymbol{q},t)$. These functions are required to satisfy

$$\left[\frac{\partial}{\partial t} + \nu(k^2+p^2+q^2)\right]\theta(\boldsymbol{k},\boldsymbol{p},\boldsymbol{q};t) = 1 - [\mu^s(\boldsymbol{k},t) + \mu^s(\boldsymbol{p},t) + \mu^s(\boldsymbol{q},t)]\theta(\boldsymbol{k},\boldsymbol{p},\boldsymbol{q};t), \tag{4.71}$$

$$\left[\frac{\partial}{\partial t} + \nu(k^2+p^2+q^2)\right]\tilde{\theta}(\boldsymbol{k},\boldsymbol{p},\boldsymbol{q};t) = 1 - [\mu^s(\boldsymbol{k},t) + \mu^s(\boldsymbol{p},t) + \mu^c(\boldsymbol{q},t)]\tilde{\theta}(\boldsymbol{k},\boldsymbol{p},\boldsymbol{q};t), \tag{4.72}$$

with the initial conditions

$$\theta(\boldsymbol{k},\boldsymbol{p},\boldsymbol{q},0) = \tilde{\theta}(\boldsymbol{k},\boldsymbol{p},\boldsymbol{q},0) = 0. \tag{4.73}$$

The damping factors are defined by

$$\mu^s(\boldsymbol{k},t) \equiv 2\sum_{\boldsymbol{p},\boldsymbol{q}\ni m_q\geqslant 0}\tilde{\theta}(\boldsymbol{p},\boldsymbol{k},\boldsymbol{q},t)|\breve{g}(\boldsymbol{p},\boldsymbol{q},\boldsymbol{k})|^2U_E(\boldsymbol{p},t), \tag{4.74}$$

$$\mu^c(\boldsymbol{k},t) \equiv 2\sum_{\boldsymbol{p},\boldsymbol{q}}\tilde{\theta}(\boldsymbol{p},\boldsymbol{q},\boldsymbol{k},t)|\breve{g}(\boldsymbol{p},\boldsymbol{k},\boldsymbol{q})|^2U_E(\boldsymbol{p},t). \tag{4.75}$$

These two turbulent eddy damping factors are clearly real functions and satisfy

$\mu^s(\boldsymbol{k},t) = \mu^s(-\boldsymbol{k},t)$ and $\mu^c(\boldsymbol{k},t) = \mu^c(-\boldsymbol{k},t)$. The function $\breve{g}$ is defined by

$$\breve{g}(\boldsymbol{p},\boldsymbol{q},\boldsymbol{k}) \equiv -\frac{\epsilon_{m_q} A^2(k,p,q)}{k\,p\,q} \sum_{s_p,s_q=\pm} \delta_{\boldsymbol{k}+\boldsymbol{p}_{s_p}+\boldsymbol{q}_{s_q},\boldsymbol{0}} \exp[i(s_p\phi_{\boldsymbol{p}_{s_p}} + \phi_{\boldsymbol{k}})_{\hat{\boldsymbol{n}}(\boldsymbol{k},\boldsymbol{p}_{s_p},\boldsymbol{q}_{s_q})}]. \quad (4.76)$$

It can be shown that

$$\breve{g}(\boldsymbol{k},\boldsymbol{p},\boldsymbol{q}) = \breve{g}(\boldsymbol{q},\boldsymbol{p},\boldsymbol{k}) = \breve{g}^*(-\boldsymbol{k},-\boldsymbol{p},-\boldsymbol{q}) = \breve{g}^*(\boldsymbol{k}_-,\boldsymbol{p}_-,\boldsymbol{q}_-). \quad (4.77)$$

See Turner (1997).

Three of these equations can be further massaged resulting in the final set that exhibits aspects of the behaviour of both our two-dimensional and three-dimensional results from the test-field model of Navier–Stokes turbulence. Thus making use of the assumed symmetry of the spectrum, U_E, under reflection of its wave-vector argument about the (x,z)-plane, we rewrite (4.70), (4.74), and (4.75) as follows:

$$\begin{aligned}\left(\frac{\partial}{\partial t} + 2\nu k^2\right) U_E(\boldsymbol{k},t) = \frac{1}{2k^2} & \sum_{\boldsymbol{p},\boldsymbol{q}\ni p_y q_y \neq 0} \delta_{\boldsymbol{q}+\boldsymbol{p},\boldsymbol{k}} \sin^2(\alpha_{\boldsymbol{k}})\theta(\boldsymbol{k},\boldsymbol{p},\boldsymbol{q};t) \\ & \times[(k^2-p^2)(q^2-p^2)+k^2q^2][U_E(\boldsymbol{q},t)-U_E(\boldsymbol{k},t)]U_E(\boldsymbol{p},t) \\ & + \frac{2}{k^2}\delta_{k_y,0} \sum_{\boldsymbol{q},\boldsymbol{p}\ni q_y=p_y=0} \delta_{q_x+p_x,k_x}\delta_{q_z+p_z,k_z} \sin^2(\alpha_{\boldsymbol{k}})\theta(\boldsymbol{k},\boldsymbol{p},\boldsymbol{q};t) \\ & \times(k^2-p^2)(q^2-p^2)[U_E(\boldsymbol{q},t)-U_E(\boldsymbol{k},t)]U_E(\boldsymbol{p},t) \\ & + \text{hybrid contributions}, \end{aligned} \quad (4.78)$$

$$\begin{aligned}\mu^s(\boldsymbol{k},t) = \frac{1}{2} & \sum_{\boldsymbol{p},\boldsymbol{q}\ni m_{\boldsymbol{q}}>0, p_y q_y \neq 0} \delta_{\boldsymbol{q}+\boldsymbol{p},\boldsymbol{k}} \left(\frac{pq}{k}\right)^2 \sin^4(\alpha_{\boldsymbol{k}})\tilde{\theta}(\boldsymbol{p},\boldsymbol{k},\boldsymbol{q};t)U_E(\boldsymbol{p},t) \\ & + \delta_{k_y,0} \sum_{\boldsymbol{q},\boldsymbol{p}\ni q_y=p_y=0} \delta_{q_x+p_x,k_x}\delta_{q_z+p_z,k_z} \left(\frac{pq}{k}\right)^2 \sin^4(\alpha_{\boldsymbol{k}})\tilde{\theta}(\boldsymbol{p},\boldsymbol{k},\boldsymbol{q};t)U_E(\boldsymbol{p},t) \\ & + \text{hybrid contributions}, \end{aligned} \quad (4.79)$$

$$\begin{aligned}\mu^c(\boldsymbol{k},t) = \frac{1}{2} & \sum_{\boldsymbol{p},\boldsymbol{q}\ni p_y q_y \neq 0} \delta_{\boldsymbol{q}+\boldsymbol{p},\boldsymbol{k}} \left(\frac{pq}{k}\right)^2 \sin^4(\alpha_{\boldsymbol{k}})\tilde{\theta}(\boldsymbol{p},\boldsymbol{q},\boldsymbol{k};t)U_E(\boldsymbol{p},t) \\ & + \delta_{k_y,0} \sum_{\boldsymbol{q},\boldsymbol{p}\ni q_y=p_y=0} \delta_{q_x+p_x,k_x}\delta_{q_z+p_z,k_z} \left(\frac{pq}{k}\right)^2 \sin^4(\alpha_{\boldsymbol{k}})\tilde{\theta}(\boldsymbol{p},\boldsymbol{q},\boldsymbol{k};t)U_E(\boldsymbol{p},t) \\ & + \text{hybrid contributions}. \end{aligned} \quad (4.80)$$

As in § 3.4, we again observe that the right-hand sides of (4.78), (4.79), and (4.80) decompose into three tantalizing sets of terms. The first set, those associated with $\boldsymbol{k}$, $\boldsymbol{p}$, and $\boldsymbol{q}$ wave vectors, all of which have non-vanishing y-components, demonstrates a three-dimensional aspect. They are virtually identical to the right-hand sides of (4.47), (4.51), and (4.52), respectively, which refer to the TFM evolution of isotropic mirror-symmetric homogeneous three-dimensional turbulence.

The second set of these terms, those associated with $\boldsymbol{k}$, $\boldsymbol{p}$, and $\boldsymbol{q}$ wave vectors, all of which have vanishing y-components, demonstrates a two-dimensional aspect.

These terms are virtually identical to the right-hand sides of (4.61), (4.64), and (4.65), which refer to the TFM evolution of isotropic mirror-symmetric homogeneous two-dimensional turbulence. (Of course, one must be careful when making correspondences between sums over a discrete set of states with integrals over a continuum of states.)

The final set of terms labelled hybrid contributions is the collection of remaining terms, those associated with $\boldsymbol{k}$, $\boldsymbol{p}$, and $\boldsymbol{q}$ wave vectors only one of which has a vanishing y-component.

We wish to re-emphasize that even when our channel-flow spectrum, $U_E(\boldsymbol{k}, t)$, is isotropic in wave-vector space, the mapping from wave-vector space back to physical space will be neither homogeneous nor isotropic!

4.4. *Summary and conclusions*

In this section, we have shown that the use of a helicity decomposition for the representation of incompressible Navier–Stokes turbulence greatly facilitates the analysis of turbulence closures. The associated compact notation, which obviates the use of solenoidal projection operators, clarifies the nonlinear coupling of the modes of the Navier–Stokes equation. This clarification is embodied in the structure function, which implicitly is a function of the Navier–Stokes modal dynamics as well as of the global geometry.

As a result, we obtained with relative ease the equations for the following closures and explored their relationships:

(i) DIA for three-dimensional homogeneous turbulence that need be neither isotropic nor mirror-symmetric;

(ii) DIA for an arbitrary two-dimensional homogeneous turbulence;

(iii) DIA for three-dimensional turbulence in a free-slip channel flow;

(iv) TFM for three-dimensional homogeneous isotropic mirror-symmetric turbulence;

(v) TFM for an arbitrary two-dimensional homogeneous turbulence;

(vi) TFM for two-dimensional isotropic homogeneous turbulence; and

(vii) TFM for three-dimensional turbulence in a free-slip channel flow.

These lead us to the following conclusions:

(i) These DIA and TFM equations for the free-slip channel flow are entirely new results. They may be compared with the EDQNM equations of § 3.4.

(ii) The evolution equations of turbulent spectra may have striking similarities in different geometries. Their different aspects in coordinate space arise entirely from the different bases used to represent the fluid velocity. These bases differ from each other due to differences in global geometry and boundary conditions.

(iii) Two-dimensional homogeneous turbulence closures are easily gleaned from the three-dimensional homogeneous closures. One merely extracts the structure functions associated with the two-dimensional cases from their three-dimensional counterparts.

(iv) The physics of these decompositions is not obscured by the presence of cumbersome projection operators. Evidence is given by the clear positivity of the coefficients of the $\tilde{\theta}$ functions in all of the TFM expressions for the turbulent eddy damping factors, μ^s and μ^c.

The compact notation of these decompositions allows the study of turbulence in finite geometries and analysis of scalings in the associated non-isotropic and inhomogeneous turbulence environments. From there, one can develop theoreticallybased engineering models. It will be interesting to study other types of closures using these decompositions.

5. Final comments

Much of this manuscript relies on interesting, extensive, and occasionally even elegant analysis that can be found in the archived manuscripts (Turner 1996*a*, *b*, 1997). If parts of this paper, such as § 4, seem to be more of a skeletal formulary, realize that the muscle that pulls it all together has been stripped and stored. In many ways the contents of this manuscript should not be of lesser importance to the interested theorist than the means necessary to derive these contents, means that is discussed exhaustively in the archived documents.

We wish to remark upon the results of this manuscript. We have shown that the strength of the helicity decomposition is its adaptability to new geometries, its compact representation of extensive physical and geometric information, and the relative ease and reliability with which it can be utilized. We have used it to write down the four independent equations describing the evolution of an arbitrary homogeneous incompressible Navier–Stokes turbulence in three dimensions with four real functions using the time-honoured EDQNM closure. We have used it to describe the evolution of Navier–Stokes turbulence in a channel within two parallel planar free-slip boundaries. By invoking a hypothesis of random phase, we were again able to utilize the EDQNM closure to describe this incompressible, inhomogeneous, anisotropic turbulence. We found aspects of our evolution equation noteworthy by virtue of their close resemblance to aspects of two-dimensional and three-dimensional homogeneous turbulence. Clearly much of the geometric information was contained in the mapping from the wave-vector space back to the physical space. We also commented that the random-phase hypothesis invoked originally in Turner (1996*b*) has received validation in recent direct numerical simulations of the Navier–Stokes equation with the channel-flow boundary conditions by Ulitsky *et al.* (1999). See also Turner & Turner (2000). In the final sections of this manuscript, we demonstrated the ease with which other closures (represented by the DIA and TFM) may be obtained in a variety of geometries using the helicity decomposition.

Thus we have described an inhomogeneous turbulence with precisely the same closure tools that have been used for the description of homogeneous turbulence, and with only the additional ingredient, now validated, of the random-phase approximation. We can describe flows that have non-vanishing gradients of quantities, such as mean pressure, mean velocity, pressure–velocity correlations, and triple-velocity correlations (Turner 1999). No longer must we confine ourselves to an assumption of weak spatial inhomogeneity in the turbulence. Our pressure is globally determined through implicitly satisfying a pressure-Poisson equation.

I am indebted to Timothy T. Clark and Charles Zemach for useful and critical discussions during this research. I am particularly grateful to Mark Ulitsky for a meticulous proofreading of the first two of the three archived documents. He also pointed out to me the necessity of separating the contributions of modes having wave vectors with vanishing y-components from the other modes in (3.39) due to the associated degeneracies. I am grateful to Harvey A. Rose for insightful comments on my use of the random-phase approximation. Finally, I wish also to thank Rena T. Fleur for her selfless dedication in painstakingly typing this manuscript.

This work was supported by the US Department of Energy and Los Alamos National Laboaratory under LDRD project #IP97-018.

REFERENCES

André, J. C. & Lesieur, M. 1977 Influence of helicity on the evolution of isotropic turbulence at high Reynolds number. *J. Fluid Mech.* **81**, 187–207.

Bertoglio, J. P. & Jeandel, D. A. 1987 A simplified spectral closure for inhomogeneous turbulence: Application to the boundary layer. In *Turbulent Shear Flows 5*, pp. 19–30. Springer.

Besnard, D. C., Harlow, F. H., Rauenzahn, R. M. & Zemach, C. 1996 Spectral transport model for turbulence. *Theor. Comput. Fluid Dyn.* **8**, 1–35.

Bohm, D. & Pines, D. 1951 A collective description of electron interactions. I. Magnetic interactions. *Phys. Rev.* **82**, 625–634.

Cambon, C. & Jacquin, L. 1989 Spectral approach to non-isotropic turbulence subjected to rotation. *J. Fluid Mech.* **202**, 295–317.

Cambon, C., Mansour, N. N. & Godeferd, F. S. 1997 Energy transfer in rotating turbulence. *J. Fluid Mech.* **337**, 303–332.

Cambon, C., Teissedre, C. & Jeandel, D. 1985 Etude d'effets couplés de déformation et de rotation sur une turbulence homogène. *J. Méc. Théor. Appl.* **4**, 629–657.

Chandrasekhar, S. & Kendall, P. C. 1957 On force-free magnetic fields. *Astrophys. J.* **126**, 457–460.

Chandrasekhar, S. & Reid, W. H. 1957 On the expansion of functions which satisfy four boundary conditions. *Proc. Natl Acad. Sci.* **43**, 521–527.

Craya, A. 1958 Contribution à l'analyse de la turbulence associée à des vitesses moyennes. Thèse dans Publications Scientifiques et Techniques, Ministère de l'Air, France.

Herring, J. R. 1974 Approach of axisymmetric turbulence to isotropy. *Phys. Fluids* **17**, 859–872.

Kraichnan, R. H. 1959 The structure of isotropic turbulence at very high Reynolds numbers. *J. Fluid Mech.* **5**, 497–543.

Kraichnan, R. H. 1971 An almost-Markovian Galilean-invariant turbulence model. *J. Fluid Mech.* **47**, 513–524.

Kraichnan, R. H. 1972 Test-field model for inhomogeneous turbulence. *J. Fluid Mech.* **56**, 287–304.

Kraichnan, R. H. 1973 Helical turbulence and absolute equilibrium. *J. Fluid Mech.* **59**, 745–752.

Leith, C. E. & Kraichnan, R. H. 1972 Predictability of turbulent flows. *J. Atmos. Sci.* **29**, 1041–1058.

Lesieur, M. 1990*a* *Turbulence in Fluids: Stochastic and Numerical Modeling*, second revised edn. Kluwer.

Lesieur, M. 1990*b* The utility and drawback of traditional approaches. In *Whither Turbulence? Turbulence at the Crossroads* (ed. J. L. Lumley), pp. 59–69. Workshop at Cornell University, Ithaca, NY, 1989. Springer.

Li, S., Montgomery, D. & Jones, W. B. 1996 Inverse cascades of angular momentum. *J. Plasma Phys.* **56**, 615–639.

Li, S., Montgomery, D. & Jones, W. B. 1997 Two-dimensional turbulence with rigid circular walls. *Theor. Comput. Fluid Dyn.* **9**, 167–181.

Montgomery, D., Turner, L. & Vahala, G. 1978 Three-dimensional magnetohydrodynamic turbulence in cylindrical geometry. *Phys. Fluids* **21**, 757–764.

Moses, H. E. 1971 Eigenfunctions of the curl operator, rotationally invariant Helmholtz theorem, and applications to electromagnetic theory and fluid mechanics. *SIAM J. Appl. Maths* **21**, 114–144.

Orszag, S. A. 1977 Lectures on the statistical theory of turbulence. In *Fluid Dynamics 1973, Les Houches Summer School of Theoretical Physics* (ed. R. Balian & J.-L. Peube), pp. 235–374. Gordon and Breach.

Schiestel, R. 1987 Multiple-time scaling of turbulent flows in one point closures. *Phys. Fluids* **30**, 722–731.

Turner, L. 1983 Statistical mechanics of a bounded, ideal magnetofluid. *Ann. Phys. NY* **149**, 58–161.

Turner, L. 1996*a* Helicity decomposition of evolution of incompressible turbulence. I. Homogeneous, anisotropic, helical case. Los Alamos Unclassified Report #LA-UR 96-618.†

Turner, L. 1996*b* Helicity decomposition of evolution of incompressible turbulence. II. Inhomogeneous case – free slip channel. Los Alamos Unclassified Report #LA-UR 96-3257.†

Turner, L. 1997 Helicity decomposition of evolution of incompressible turbulence. III. Direct-interaction approximation and test-field models of two- and three-dimensional homogeneous and free-slip channel cases. Los Alamos Unclassified Report #LA-UR 97-339.†

Turner, L. 1999 Macroscopic structures of inhomogeneous, Navier–Stokes turbulence. *Phys. Fluids* **11**, 2367–2380.

Turner, L. & Christiansen, J. P. 1981 Incomplete relaxation of pinch discharges. *Phys. Fluids* **24**, 893–898.

Turner, A. M. & Turner, L. 2000 Manifestation of random phase in a finite ensemble of a turbulent fluid. *Phys. Rev. Lett*. **84**, 1176–1179.

Ulitsky, M., Clark, T. & Turner, L. 1999 Testing a random phase approximation for bounded turbulent flow. *Phys. Rev.* E **59**, 5511–5522.

Waleffe, F. 1992 The nature of triad interactions in homogeneous turbulence. *Phys. Fluids* A **4**, 350–363.

Waleffe, F. 1993 Inertial transfers in the helical decomposition. *Phys. Fluids* A **5**, 677–685.

† Archived in the Editorial Office of the *Journal of Fluid Mechanics*, and copies are available on request.